



CTRQ 2022

The Fifteenth International Conference on Communication Theory, Reliability, and
Quality of Service

ISBN: 978-1-61208-944-7

April 24 - 28, 2022

Barcelona, Spain

CTRQ 2022 Editors

Pascal Lorenz, University of Haute-Alsace, France

CTRQ 2022

Forward

The Fifteenth International Conference on Communication Theory, Reliability, and Quality of Service (CTRQ 2022) continued a series of events focusing on the achievements on communication theory with respect to reliability and quality of service. The conference also dealt with the most recent results in theory and practice on improving network and system reliability, as well as new mechanisms related to quality of service tuned to user profiles.

The processing and transmission speed and increasing memory capacity might be a satisfactory solution on the resources needed to deliver ubiquitous services, under guaranteed reliability and satisfying the desired quality of service. Successful deployment of communication mechanisms guarantees a decent network stability and offers a reasonable control on the quality of service expected by the end users. Recent advances on communication speed, hybrid wired/wireless, network resiliency, delay-tolerant networks and protocols, signal processing and so forth asked for revisiting some aspects of the fundamentals in communication theory. Mainly network and system reliability and quality of service are those that affect the maintenance procedures, on the one hand, and the user satisfaction on service delivery, on the other hand. Reliability assurance and guaranteed quality of services require particular mechanisms that deal with dynamics of system and network changes, as well as with changes in user profiles. The advent of content distribution, IPTV, video-on-demand and other similar services accelerate the demand for reliability and quality of service.

We take here the opportunity to warmly thank all the members of the CTRQ 2022 technical program committee, as well as all the reviewers. The creation of such a high-quality conference program would not have been possible without their involvement. We also kindly thank all the authors who dedicated much of their time and effort to contribute to CTRQ 2022. We truly believe that, thanks to all these efforts, the final conference program consisted of top-quality contributions. We also thank the members of the CTRQ 2022 organizing committee for their help in handling the logistics of this event.

CTRQ 2022 Chairs

CTRQ 2022 Steering Committee

Kiran Makhijani, FutureWei, USA

Daniele Codetta Raiteri, Università del Piemonte Orientale, Italy

Ali Jalooli, California State University at Dominguez Hills, USA

Costas Vassilakis, University of the Peloponnese – Tripoli, Greece

CTRQ 2022 Publicity Chairs

Javier Rocher, Universitat Politècnica de València, Spain

Lorena Parra, Universitat Politècnica de València, Spain

CTRQ 2022 Committee

CTRQ 2022 Steering Committee

Kiran Makhijani, FutureWei, USA
Daniele Codetta Raiteri, Università del Piemonte Orientale, Italy
Ali Jalooli, California State University at Dominguez Hills, USA
Costas Vassilakis, University of the Peloponnese – Tripoli, Greece

CTRQ 2022 Publicity Chairs

Javier Rocher, Universitat Politècnica de València, Spain
Lorena Parra, Universitat Politècnica de València, Spain

CTRQ 2022 Technical Program Committee

Sami Marzook Alesawi, King Abdulaziz University, KSA
Michael Atighetchi, Raytheon BBN, USA
Jasmina Barakovic Husic, BH Telecom, Joint Stock Company / University of Sarajevo, Bosnia and Herzegovina
Sara Berri, CY Cergy Paris University | ENSEA | CNRS, France
Eugen Borcoci, University Politehnica of Bucharest, Romania
Christos Bouras, University of Patras, Greece
Hao Che, University of Texas at Arlington, USA
Daniele Codetta-Raiteri, Università del Piemonte Orientale, Italy
Rita Girao-Silva, University of Coimbra & INESC-Coimbra, Portugal
Apostolos Gkamas, University Ecclesiastical Academy of Vella of Ioannina, Greece
Lucian Grigorie, Military Technical Academy "Ferdinand I", Bucharest, Romania
Lav Gupta, University of Missouri - St. Louis, USA
Ilias Iliadis, IBM Research - Zurich, Switzerland
Ali Jalooli, California State University Dominguez Hills, USA
Jinlei Jiang, Tsinghua University, China
Laxima Niure Kandel, Embry-Riddle Aeronautical University, USA
Sokratis K. Katsikas, Norwegian University of Science and Technology, Norway
Ajey Kumar, Symbiosis Centre for Information Technology, India
Mikel Larrea, University of the Basque Country UPV/EHU, Spain
Dengzhi Liu, Jiangsu Ocean University, China
Sassi Maaloul, Higher Communications School of Tunis (SUP'COM), Tunisia
Kiran Makhijani, FutureWei, USA
Zoubir Mammeri, IRIT - Paul Sabatier University, Toulouse, France
Glenford Mapp, Middlesex University, UK
Amalia Miliou, Aristotle University of Thessaloniki, Greece
Ricky Mok, CAIDA/UC San Diego, USA
Salvatore Monteleone, University of Catania, Italy
Serban Georgica Obreja, University Politehnica Bucharest, Romania
Danda B. Rawat, Howard University, USA
Adib Rastegarnia, Purdue University, USA
Karim Mohammed Rezaul, Wrexham Glyndŵr University, UK
Abdulhakim Sabur, Arizona State University, USA

Nico Saputro, Parahyangan Catholic University, Bandung, Indonesia
Hafiz Muhammad Faisal Shehzad, University Technology Malaysia, Johor, Malaysia
Stavros Shiaeles, University of Portsmouth, UK
Vasco N. G. J. Soares, Instituto de Telecomunicações / Instituto Politécnico de Castelo Branco, Portugal
Eirini Eleni Tsiropoulou, University of New Mexico, USA
Dalton C. G. Valadares, Federal Institute of Pernambuco (IFPE), Brazil
Costas Vassilakis, University of the Peloponnese, Greece
You-Chiun Wang, National Sun Yat-sen University, Taiwan
Daqing Yun, Harrisburg University, USA
Ruochen Zeng, Marvell Semiconductor, USA
Qi Zhao, UCLA, USA
Belhassen Zouari, SupCom | University of Carthage, Tunisia

Copyright Information

For your reference, this is the text governing the copyright release for material published by IARIA.

The copyright release is a transfer of publication rights, which allows IARIA and its partners to drive the dissemination of the published material. This allows IARIA to give articles increased visibility via distribution, inclusion in libraries, and arrangements for submission to indexes.

I, the undersigned, declare that the article is original, and that I represent the authors of this article in the copyright release matters. If this work has been done as work-for-hire, I have obtained all necessary clearances to execute a copyright release. I hereby irrevocably transfer exclusive copyright for this material to IARIA. I give IARIA permission to reproduce the work in any media format such as, but not limited to, print, digital, or electronic. I give IARIA permission to distribute the materials without restriction to any institutions or individuals. I give IARIA permission to submit the work for inclusion in article repositories as IARIA sees fit.

I, the undersigned, declare that to the best of my knowledge, the article does not contain libelous or otherwise unlawful contents or invading the right of privacy or infringing on a proprietary right.

Following the copyright release, any circulated version of the article must bear the copyright notice and any header and footer information that IARIA applies to the published article.

IARIA grants royalty-free permission to the authors to disseminate the work, under the above provisions, for any academic, commercial, or industrial use. IARIA grants royalty-free permission to any individuals or institutions to make the article available electronically, online, or in print.

IARIA acknowledges that rights to any algorithm, process, procedure, apparatus, or articles of manufacture remain with the authors and their employers.

I, the undersigned, understand that IARIA will not be liable, in contract, tort (including, without limitation, negligence), pre-contract or other representations (other than fraudulent misrepresentations) or otherwise in connection with the publication of my work.

Exception to the above is made for work-for-hire performed while employed by the government. In that case, copyright to the material remains with the said government. The rightful owners (authors and government entity) grant unlimited and unrestricted permission to IARIA, IARIA's contractors, and IARIA's partners to further distribute the work.

Table of Contents

Effect of Lazy Rebuild on Reliability of Erasure-Coded Storage Systems <i>Ilias Iliadis</i>	1
Explaining Radio Access Network User Dissatisfaction with Multiple Regression Models <i>Adrien Schaffner, Louise Trave-Massuyes, Simon Pachy, and Bertrand Le Marec</i>	11

Effect of Lazy Rebuild on Reliability of Erasure-Coded Storage Systems

Ilias Iliadis

IBM Research Europe – Zurich
8803 Rüschlikon, Switzerland
email: ili@zurich.ibm.com

Abstract—Erasure-coding redundancy schemes are employed to ensure improved reliability of storage systems against device failures. The effect of the lazy rebuild scheme on the Mean Time to Data Loss (MTTDL) and the Expected Annual Fraction of Data Loss (EAFDL) reliability metrics is evaluated. A theoretical model that considers the effect of latent errors and device failures is developed. Analytical reliability expressions for the symmetric, clustered, and declustered data placement schemes are derived. It is demonstrated that the employment of lazy rebuild results in a reliability degradation of orders of magnitude. Independently of whether lazy rebuild is used, for realistic values of sector error rates, the results obtained demonstrate that MTTDL degrades, whereas EAFDL remains practically unaffected. It is also shown that the declustered data placement scheme offers superior reliability.

Keywords—Storage; Deferred recovery or repair; Unrecoverable or latent sector errors; Reliability analysis; MTTDL; EAFDL; RAID; MDS codes; stochastic modeling.

I. INTRODUCTION

Efficient erasure coding schemes that provide high data reliability are employed in today's large-scale data storage systems to recover data lost due to device and component failures. Special cases of erasure codes are the replication schemes and the Redundant Arrays of Inexpensive Disks (RAID) schemes, such as RAID-5 and RAID-6, which have been deployed extensively in the past thirty years [1-4]. Modern storage systems though use advanced, powerful erasure coding schemes that offer high storage efficiency and improve data reliability [5-8]. The reliability of storage systems is also improved by employing a declustered data placement scheme, but is adversely affected by latent or unrecoverable sector errors that are discovered when there is an attempt to access these sectors [9]. Permanent losses of data due to latent errors are quite pronounced in higher-capacity HDDs and storage nodes [10-12].

Despite the reduction in storage overhead and the improvement of reliability achieved, erasure coding is hindered from becoming more pervasive in large-scale distributed storage systems by the *repair problem*. This issue arises from the increased network traffic needed to repair data lost due to device failures and generated by the downloads and disk IOPS performed during the data recovery process [6][7][13]. To cope with the repair problem and reduce the amount of data transmitted during rebuilds, a lazy rebuild scheme was proposed in [14]. A careful scheduling of rebuild operations substantially reduces recovery bandwidth, while keeping the impact on read performance and data durability low. Lazy recovery reduces repair bandwidth at the expense of increasing

the amount of degraded stripes, which in turn affects system reliability. The lazy recovery scheme bears some similarity to the practice of delaying recovery of failed nodes by a fixed amount of time (typically 15 minutes) to avoid unnecessary repairs of short transient failures [5]. The main difference, however, is that a lazy repair is initiated based on the state of the system and does not depend on the time that has elapsed after a node failure. This results in transferring less data than the delayed recovery scheme.

The key contributions of this article are the following. We consider the reliability of erasure-coded storage systems when a lazy rebuild scheme is employed and derive closed-form expressions for the MTTDL and EAFDL reliability metrics for the symmetric, clustered, and declustered data placement schemes. We adopt the non-Markovian methodology developed in prior work [15-17] to evaluate MTTDL and EAFDL of storage systems. The validity of this methodology for accurately assessing the reliability of storage systems has been confirmed by simulations in several contexts [3][15][18][19]. It has been demonstrated that theoretical predictions of the reliability of systems comprising highly reliable storage devices are in good agreement with simulation results. Consequently, the emphasis of the present work is on theoretically assessing the effect of lazy rebuilds on the reliability of storage systems. We extend the reliability model presented in [9] to take into account lazy rebuilds. The model developed is relevant and realistic because it properly captures the characteristics of erasure coding and of the rebuild process associated with the declustered placement scheme currently used by Google [5], Microsoft Azure [7], Facebook [13], and DELL/EMC [20]. The theoretical reliability results obtained here can be used to determine the parameter values that ensure a desired level of reliability. They can also be used to assess system reliability when scrubbing is employed by applying the methodology described in [21]. We subsequently use these results to demonstrate the effect of latent errors and system parameters on system reliability.

The remainder of the article is organized as follows. Section II describes the storage system model and the corresponding parameters considered. Section III presents the general framework and methodology for deriving the MTTDL and EAFDL metrics analytically for the case of erasure-coded systems that employ a lazy rebuild scheme. Closed-form expressions for relevant reliability metrics are derived for the symmetric, clustered, and declustered data placement schemes. Section IV presents numerical results demonstrating the effectiveness of erasure coding schemes for improving system reliability as well as the adverse effect of lazy rebuilds.

TABLE I. NOTATION OF SYSTEM PARAMETERS

Parameter	Definition
n	number of storage devices
c	amount of data stored on each device
l	number of user-data symbols per codeword ($l \geq 1$)
m	total number of symbols per codeword ($m > l$)
(m, l)	MDS-code structure
d	lazy rebuild threshold ($0 \leq d < m - l$)
s	symbol size
k	spread factor of the data placement scheme, or group size (number of devices in a group) ($m \leq k \leq n$)
b	average reserved rebuild bandwidth per device
B_{\max}	upper limitation of the average network rebuild bandwidth
X	time required to read (or write) an amount c of data at an average rate b from (or to) a device
$F_X(\cdot)$	cumulative distribution function of X
$F_\lambda(\cdot)$	cumulative distribution function of device lifetimes
P_{bit}	probability of an unrecoverable bit error
s_{eff}	storage efficiency of redundancy scheme ($s_{\text{eff}} = l/m$)
U	amount of user data stored in the system ($U = s_{\text{eff}} n c$)
\tilde{r}	MDS-code distance: minimum number of codeword symbols lost that lead to permanent data loss ($\tilde{r} = m - l + 1$ and $2 \leq \tilde{r} \leq m$)
C	number of symbols stored in a device ($C = c/s$)
μ^{-1}	mean time to read (or write) an amount c of data at an average rate b from (or to) a device ($\mu^{-1} = E(X) = c/b$)
λ^{-1}	mean time to failure of a storage device ($\lambda^{-1} = \int_0^\infty [1 - F_\lambda(t)] dt$)
P_s	probability of an unrecoverable sector (symbol) error
P_{DL}	probability of data loss during rebuild
P_{UF}	probability of data loss due to unrecoverable failures during rebuild
P_{DF}	probability of data loss due to a disk failure during rebuild
Q	amount of lost user data during rebuild
H	amount of lost user data, given that data loss has occurred, during rebuild
S	number of lost symbols during rebuild

Finally, we conclude in Section V.

II. STORAGE SYSTEM MODEL

Here we briefly review the operational characteristics of erasure-coded storage systems. To assess their reliability, we adopt the model used in [9] and extend it to cover the case of lazy rebuilds. The storage system comprises n storage devices (nodes or disks), where each device stores an amount c of data such that the total storage capacity of the system is nc . This does not account for the spare space used by the rebuild process.

User data is divided into blocks of fixed size s and complemented with parity symbols to form codewords. Maximum Distance Separable (MDS) erasure codes (m, l) that map l user-data symbols to codewords of m symbols are employed. They have the property that any subset containing l of the m codeword symbols can be used to reconstruct (recover) a codeword. The corresponding storage efficiency s_{eff} and amount U of user data stored in the system is

$$s_{\text{eff}} = l/m \quad \text{and} \quad U = s_{\text{eff}} n c = l n c / m. \quad (1)$$

Also, the number C of symbols stored in a device is

$$C = c/s. \quad (2)$$

Our notation is summarized in Table I. The derived parameters are listed in the lower part of the table. To minimize the risk of permanent data loss, the m symbols of each codeword are spread and stored on m distinct devices. This way, the system can tolerate any $\tilde{r} - 1$ device failures, but \tilde{r} device failures may lead to data loss, with

$$\tilde{r} = m - l + 1, \quad 1 \leq l < m \quad \text{and} \quad 2 \leq \tilde{r} \leq m. \quad (3)$$

Examples of MDS erasure codes are the replication, RAID-5, RAID-6, and Reed–Solomon schemes.

Data is stored according to symmetric placement schemes, including the *clustered* and *declustered* placement schemes, as shown in Figure 1 of [9][17]. The system comprises n/k disjoint groups of k devices. Within each group, all $\binom{k}{m}$ possible ways of placing m symbols across k devices are used equally to store all the codewords in that group. Refer to [9] for additional details.

A. Codeword Reconstruction and Rebuild Process

When storage devices fail, codewords lose some of their symbols, and this reduces data redundancy. The system attempts to maintain its redundancy by reconstructing the lost codeword symbols using the surviving symbols of the affected codewords. As the times to detect device failures are much shorter than rebuild times, we assume that failures are detected instantaneously. When a *lazy rebuild* scheme is used, the rebuild process is not triggered immediately, but is delayed until additional device failures occur that result in d additional symbol losses within some of the codewords. Consequently, the rebuild process is initiated when codewords have lost $1 + d$ symbols. To avoid permanent data losses, the number of symbols lost within codewords should be less than the MDS-code distance \tilde{r} , that is, this number should not exceed $\tilde{r} - 1$, which implies that $d + 1 \leq \tilde{r} - 1 = m - l$. Thus, we have

$$l < m \leq k \leq n \quad (n/k \in \mathbb{N}) \quad \text{and} \quad 0 \leq d \leq m - l - 1. \quad (4)$$

1) *Exposure Levels*: The system is at exposure level u ($0 \leq u \leq \tilde{r}$) when there are codewords that have lost u symbols owing to device failures, but there are no codewords that have lost more symbols. These codewords are referred to as the *most-exposed* codewords. Transitions to higher exposure levels are caused by device failures, whereas transitions to lower ones are caused by successful rebuilds. We denote by C_u the number of most-exposed codewords upon entering exposure level u , ($u \geq 1$). Upon the first device failure it holds that

$$C_1 = C, \quad (5)$$

where C is determined by (2). In Section III, we will derive the reliability metrics of interest using the *direct path approximation*, which considers only transitions from lower to higher exposure levels [3][15][18][19][22]. This implies that each exposure level is entered only once.

2) *Prioritized Lazy Rebuild*: When a symmetric or declustered placement scheme is used, as shown in Figure 2 of [9][17], spare space is reserved on each device for temporarily storing the reconstructed codeword symbols before they are transferred to a new replacement device. The rebuild process to restore the data lost by failed devices is assumed to be both *prioritized* and *distributed*. A prioritized (or intelligent) rebuild process always attempts first to rebuild the *most-exposed* codewords, namely, the codewords that have lost the largest number of symbols [3][5][7][14][17][18]. According to the lazy rebuild scheme, no recovery actions are performed at exposure levels u not exceeding the threshold d . However, when the system enters a higher exposure level u , the rebuild process is triggered and attempts to bring the system back to exposure level $u - 1$ by reading l symbols and recovering one of the u symbols that each of the C_u most-exposed codewords

has lost. To improve reliability, the vulnerability window is reduced by recovering only one symbol as opposed to the scheme considered in [14] that recovers multiple symbols. In a distributed rebuild process, the codewords are reconstructed by reading symbols from an appropriate set of surviving devices and storing the recovered symbols in the reserved spare space of these devices. During this process, it is desirable to reconstruct the lost codeword symbols on devices in which another symbol of the same codeword is not already present.

In the case of clustered placement, the codeword symbols are spread across all k ($= m$) devices in each group (cluster). Therefore, reconstructing the lost symbols on the surviving devices of a group would result in more than one symbol of the same codeword on the same device. To avoid this, the lost symbols are reconstructed directly in spare devices as described and shown in Figure 3 of [17].

3) *Rebuild Process*: A certain portion of the device bandwidth is reserved for read/write data recovery during the rebuild process, and the remaining bandwidth is used to serve user requests. Let b denote the actual average reserved rebuild bandwidth per device. Lost symbols are rebuilt in parallel using the rebuild bandwidth b available on each surviving device. The amount of data corresponding to the number C_u of symbols to be rebuilt at exposure level u is written at an average rate b_u ($\leq b$) to selected device(s). For the time X required to read (or write) an amount c of data from (or to) a device it holds that

$$\mu^{-1} \triangleq E(X) = c/b. \quad (6)$$

4) *Failure and Rebuild Time Distributions*: The lifetimes of the n devices are assumed to be independent and identically distributed, with a cumulative distribution function $F_\lambda(\cdot)$ and a mean of $1/\lambda$. The results in this article hold for *highly reliable* storage devices, which satisfy the condition [17][19]

$$\mu \int_0^\infty F_\lambda(t)[1 - F_X(t)]dt \ll 1, \quad \text{with } \frac{\lambda}{\mu} \ll 1. \quad (7)$$

5) *Amount of Data to Rebuild and Rebuild Times at Each Exposure Level*: We denote by \tilde{n}_u the number of devices at exposure level u whose failure causes an exposure level transition to level $u + 1$, and V_u the fraction of the C_u most-exposed codewords that have a symbol stored on any given such device. Note that \tilde{n}_u depends on the codeword placement scheme. Let R_u denote the rebuild time of the most-exposed codewords at exposure level u and α_u be the fraction of the rebuild time R_u still left when another device fails, causing the exposure level transition $u \rightarrow u + 1$. For $u \leq d$, no rebuild is performed and therefore $\alpha_u = 1$. For $u > d$, α_u is approximately uniformly distributed in $(0, 1)$ [23, Lemma 2]. Therefore,

$$\alpha_u \approx \begin{cases} 1, & \text{for } u = 1, \dots, d \\ U(0, 1), & \text{for } u = d + 1, \dots, \tilde{r} - 1. \end{cases} \quad (8)$$

We proceed by considering that the rebuild time R_{u+1} is determined completely by R_u and α_u in the same manner as in [16][17][22]. For the rebuild schemes considered, the fraction of the C_u most-exposed codewords that were not yet considered by the rebuild process upon the next device failure is roughly equal to the fraction α_u of the rebuild time R_u still left. Therefore, upon the next device failure, an approximate

number $\alpha_u C_u$ of the C_u codewords were not yet considered by the rebuild process. Clearly, the fraction V_u of these codewords that have symbols stored on the newly failed device depends only on the codeword placement scheme. Consequently, the number C_{u+1} of the most-exposed codewords upon entering exposure level $u + 1$ is

$$C_{u+1} \approx V_u \alpha_u C_u, \quad \text{for } u = 1, \dots, \tilde{r} - 1. \quad (9)$$

Repeatedly applying (9) and using (5) and the convention that for any sequence δ_i , $\prod_{i=1}^0 \delta_i \triangleq 1$, yields

$$C_u \approx C \prod_{i=1}^{u-1} V_i \alpha_i, \quad \text{for } u = 1, \dots, \tilde{r}. \quad (10)$$

6) *Unrecoverable Errors*: The reliability of storage systems is affected by the occurrence of unrecoverable or latent errors. Let P_{bit} denote . According to the specifications, the unrecoverable bit-error probability P_{bit} is equal to 10^{-15} for SCSI drives and 10^{-14} for SATA drives [21]. Assuming that bit errors occur independently over successive bits, the unrecoverable sector (symbol) error probability P_s is

$$P_s = 1 - (1 - P_{\text{bit}})^s, \quad (11)$$

with s expressed in bits. Assuming a sector size of 512 bytes, the equivalent unrecoverable sector error probability is $P_s \approx P_{\text{bit}} \times 4096$, which is 4.096×10^{-12} in the case of SCSI and 4.096×10^{-11} in the case of SATA drives. In practice, however, and also owing to the accumulation of latent errors over time, these probability values are higher. Indeed, empirical field results suggest that the actual values can be orders of magnitude higher, reaching $P_s \approx 5 \times 10^{-9}$ [24].

III. DERIVATION OF MTTDL AND EAFDL

The reliability metrics are derived using the direct-path-approximation methodology presented in [9][15][16][17] and extending it to assess the effect of lazy rebuilds.

At any point in time, the system is in one of two modes: non-rebuild or rebuild mode. Note that part of the non-rebuild mode is the normal mode of operation where all devices are operational and all data in the system has the original amount of redundancy. In the context of lazy rebuild, when the first device fails, the system does not enter the rebuild mode. Subsequently, we refer to the device failure that causes the transition from non-rebuild to rebuild mode as an *initial device* failure, which should not be confused with the first device failure. Consequently, an *initial device* failure triggers a rebuild process that attempts to restore the lost data, which eventually leads the system either to a Data Loss (DL) with probability P_{DL} or back to the original normal mode by restoring initial redundancy, with probability $1 - P_{\text{DL}}$.

Let T be a typical interval of a non-rebuild period, that is, the time interval from the time the system is brought to its original state until a subsequent initial device failure occurs that causes the system to enter exposure level $d + 1$. It then holds that $T = \sum_{u=0}^d T_u$, where T_0 denotes the time interval from the time the system is brought to its original state until the first device failure and T_u denotes the time that the system spends at exposure level u . For a system comprising n devices with a mean time to failure of a device equal to $1/\lambda$, it holds that $E(T_0) = 1/(n\lambda)$. Given that the number of devices

at exposure level u whose failure causes an exposure level transition to level $u+1$ is \tilde{n}_u , it holds that $E(T_u) = 1/(\tilde{n}_u \lambda)$. From the above, it follows that

$$E(T) = \sum_{u=0}^d E(T_u) = \left(\sum_{u=0}^d \frac{1}{\tilde{n}_u} \right) / \lambda, \quad \text{where } \tilde{n}_0 \triangleq n, \quad (12)$$

where \tilde{n}_u is determined by (35) or (38).

The MTTDL metric is then obtained by [15, Eq. (5)]:

$$\text{MTTDL} \approx \frac{E(T)}{P_{\text{DL}}}. \quad (13)$$

The EAFDL is obtained as the ratio of the expected amount $E(Q)$ of lost user data, normalized to the amount U of user data, to the expected duration of T [15, Eq. (9)]:

$$\text{EAFDL} \approx \frac{E(Q)}{E(T) \cdot U} \stackrel{(1)}{=} \frac{m E(Q)}{n l c E(T)}. \quad (14)$$

where $E(T)$ is determined by (12) and expressed in years.

The expected amount $E(H)$ of lost user data, given that data loss has occurred, is determined by [15, Eq. (8)]:

$$E(H) = \frac{E(Q)}{P_{\text{DL}}}. \quad (15)$$

A. Reliability Analysis

The reliability evaluation of the lazy rebuild scheme is based on the reliability analysis presented in [9]. The MTTDL and EAFDL reliability metrics were determined by first deriving the probability of data loss P_{DL} and the expected amount $E(Q)$ of lost user data. Central to these derivations are the variables α_u that represent the fractions of the rebuild times R_u still left when device failures cause exposure level transitions. These variables were assumed to be independent and approximately uniformly distributed in $(0, 1)$. However, in the case of lazy rebuild, these variables are distributed according to (8). We now proceed to derive the various measures of interest.

At any exposure level u ($u = d+1, \dots, \tilde{r}-1$), data loss may occur during rebuild owing to one or more unrecoverable failures, which is denoted by the transition $u \rightarrow \text{UF}$. Moreover, at exposure level $\tilde{r}-1$, data loss occurs owing to a subsequent device failure, which leads to the transition to exposure level \tilde{r} . Consequently, the direct paths that lead to data loss are the following:

\overrightarrow{UF}_u : the direct path of successive transitions $1 \rightarrow 2 \rightarrow \dots \rightarrow u \rightarrow \text{UF}$, for $u = d+1, \dots, \tilde{r}-1$, and

\overrightarrow{DF} : the direct path of successive transitions $1 \rightarrow 2 \rightarrow \dots \rightarrow \tilde{r}-1 \rightarrow \tilde{r}$,

with corresponding probabilities P_{UF_u} and P_{DF} , respectively.

1) *Data Loss*: It holds that

$$P_{\text{UF}_u} = P_u P_{u \rightarrow \text{UF}}, \quad \text{for } u = d+1, \dots, \tilde{r}-1, \quad (16)$$

where P_u is the probability of entering exposure level u , which is derived in Appendix A as follows:

$$P_u \approx \frac{(\lambda c \prod_{j=1}^d V_j)^{u-d-1}}{(u-d-1)!} \frac{E(X^{u-d-1})}{[E(X)]^{u-d-1}} \prod_{i=d+1}^{u-1} \frac{\tilde{n}_i}{b_i} V_i^{u-1-i}, \quad (17)$$

and $P_{u \rightarrow \text{UF}}$ is the probability of encountering an unrecoverable failure during the rebuild process at this exposure level.

In [25], it was shown that P_{DL} is accurately approximated by the probability of all direct paths to data loss. Therefore,

$$P_{\text{DL}} \approx P_{\text{DF}} + \sum_{u=d+1}^{\tilde{r}-1} P_{\text{UF}_u}. \quad (18)$$

Approximate expressions for the probabilities of data loss P_{UF_u} and P_{DF} are subsequently obtained by the following proposition.

Proposition 1: For $u = d+1, \dots, \tilde{r}-1$, it holds that

$$\begin{aligned} P_{\text{UF}_u} &\approx - \left(\lambda c \prod_{j=1}^d V_j \right)^{u-d-1} \frac{E(X^{u-d-1})}{[E(X)]^{u-d-1}} \left(\prod_{i=d+1}^{u-1} \frac{\tilde{n}_i}{b_i} V_i^{u-1-i} \right) \\ &\quad \cdot \log(\hat{q}_u)^{-(u-d-1)} \left(\hat{q}_u - \sum_{i=0}^{u-d-1} \frac{\log(\hat{q}_u)^i}{i!} \right), \end{aligned} \quad (19)$$

where

$$\hat{q}_u \triangleq q_u^{C \prod_{j=1}^{u-1} V_j}, \quad (20)$$

$$q_u = 1 - \sum_{j=\tilde{r}-u}^{m-u} \binom{m-u}{j} P_s^j (1-P_s)^{m-u-j}, \quad (21)$$

$$P_{\text{DF}} \approx \frac{(\lambda c \prod_{j=1}^d V_j)^{\tilde{r}-d-1}}{(\tilde{r}-d-1)!} \frac{E(X^{\tilde{r}-d-1})}{[E(X)]^{\tilde{r}-d-1}} \prod_{i=d+1}^{\tilde{r}-1} \frac{\tilde{n}_i}{b_i} V_i^{\tilde{r}-1-i}. \quad (22)$$

Proof: Equation (19) is obtained in Appendix A. Equation (22) is obtained from the fact that $P_{\text{DF}} = P_{\tilde{r}}$ and, subsequently, from (17) by setting $u = \tilde{r}$. ■

The MTTDL metric is obtained by substituting (18) into (13) as follows:

$$\text{MTTDL} \approx \frac{E(T)}{P_{\text{DF}} + \sum_{u=d+1}^{\tilde{r}-1} P_{\text{UF}_u}}, \quad (23)$$

where $E(T)$, P_{UF_u} and P_{DF} are determined by (12), (19), and (22), respectively.

2) *Amount of Data Loss*: We proceed to derive the amount of data loss during rebuild. Let Q , H , and S be the amount of lost user data, the conditional amount of lost user data, given that data loss has occurred, and the number of lost symbols, respectively. Let also Q_{DF} and Q_{UF_u} denote the amount of lost user data associated with the direct paths \overrightarrow{DF} and \overrightarrow{UF}_u , respectively. Similarly, we consider the variables H_{DF} , H_{UF_u} , S_{DF} , and S_{UF_u} . Then, the amount Q of lost user data is obtained by

$$Q \approx \begin{cases} H_{\text{DF}}, & \text{if } \overrightarrow{DF} \\ H_{\text{UF}_u}, & \text{if } \overrightarrow{UF}_u, \text{ for } u = d+1, \dots, \tilde{r}-1 \\ 0, & \text{otherwise.} \end{cases} \quad (24)$$

$$\text{Thus, } E(Q) \approx P_{\text{DF}} E(H_{\text{DF}}) + \sum_{u=d+1}^{\tilde{r}-1} P_{\text{UF}_u} E(H_{\text{UF}_u}) \quad (25)$$

$$= E(Q_{\text{DF}}) + \sum_{u=d+1}^{\tilde{r}-1} E(Q_{\text{UF}_u}), \quad (26)$$

$$\text{where } E(Q_{\text{DF}}) = P_{\text{DF}} E(H_{\text{DF}}), \quad (27)$$

$$\text{and } E(Q_{\text{UF}_u}) = P_{\text{UF}_u} E(H_{\text{UF}_u}), \quad u = d+1, \dots, \tilde{r}-1. \quad (28)$$

Note that the expected amount $E(Q)$ of lost user data is equal to the product of the storage efficiency and the expected amount of lost data, where the latter is equal to the product of the expected number of lost symbols $E(S)$ and the symbol size s . Consequently, it follows from (1) that

$$E(Q) = \frac{l}{m} E(S) s \stackrel{(2)}{=} \frac{l}{m} \frac{E(S)}{C} c. \quad (29)$$

$$\text{Similarly, } E(Q_{\text{DF}}) = \frac{l}{m} E(S_{\text{DF}}) s \stackrel{(2)}{=} \frac{l}{m} \frac{E(S_{\text{DF}})}{C} c, \quad (30)$$

$$\text{and } E(Q_{\text{UF}_u}) = \frac{l}{m} E(S_{\text{UF}_u}) s \stackrel{(2)}{=} \frac{l}{m} \frac{E(S_{\text{UF}_u})}{C} c. \quad (31)$$

Proposition 2: For $u = d+1, \dots, \tilde{r}-1$, it holds that

$$E(Q_{\text{UF}_u}) \approx c \frac{l\tilde{r}}{m} \frac{\left(\lambda c \prod_{j=1}^d V_j\right)^{u-d-1}}{(u-d)!} \frac{E(X^{u-d-1})}{[E(X)]^{u-d-1}} \left(\prod_{j=1}^d V_j\right) \cdot \left(\prod_{i=d+1}^{u-1} \frac{\tilde{n}_i}{b_i} V_i^{u-i}\right) \binom{m-u}{\tilde{r}-u} P_s^{\tilde{r}-u}, \quad P_s \ll \frac{1}{m-\tilde{r}}, \quad (32)$$

$$E(Q_{\text{DF}}) \approx c \frac{l\tilde{r}}{m} \left(\lambda c \prod_{j=1}^d V_j\right)^{\tilde{r}-d-1} \frac{1}{(\tilde{r}-d)!} \frac{E(X^{\tilde{r}-d-1})}{[E(X)]^{\tilde{r}-d-1}} \cdot \left(\prod_{j=1}^d V_j\right) \left(\prod_{i=d+1}^{\tilde{r}-1} \frac{\tilde{n}_i}{b_i} V_i^{\tilde{r}-i}\right). \quad (33)$$

Proof: Equation (32) is obtained in Appendix B. Equation (33) is obtained from (32) by setting $u = \tilde{r}$. ■

The EAFDL metric is obtained by substituting (26) into (14) as follows:

$$\text{EAFDL} \approx \frac{m[E(Q_{\text{DF}}) + \sum_{u=d+1}^{\tilde{r}-1} E(Q_{\text{UF}_u})]}{n l c E(T)}, \quad (34)$$

where $E(Q_{\text{UF}_u})$ and $E(Q_{\text{DF}})$ are determined by (32) and (33), respectively, and $E(T)$ by (12) and expressed in years.

The conditional amount $E(H)$ of lost user data, given that data loss has occurred, is obtained from (15), P_{DL} is determined by (18), (19), and (22), and $E(Q)$ is determined by (26), (32), and (33).

B. Symmetric and Declustered Placement

We consider the case $m < k \leq n$. The special case $k = m$ corresponding to the clustered placement has to be considered separately for the reasons discussed in Section II-A2. At each exposure level u , for $u = 1, \dots, \tilde{r}-1$, it holds that [16][17]

$$\tilde{n}_u^{\text{sym}} = k - u, \quad (35)$$

$$b_u^{\text{sym}} = \frac{\min((k-u)b, B_{\text{max}})}{l+1}, \quad (36)$$

$$V_u^{\text{sym}} = \frac{m-u}{k-u}. \quad (37)$$

The corresponding parameters $\tilde{n}_u^{\text{declus}}$, b_u^{declus} , and V_u^{declus} for the declustered placement are derived from (35), (36), and (37) by setting $k = n$.

C. Clustered Placement

At each exposure level u , for $u = 1, \dots, \tilde{r}-1$, it holds that [16][17]

$$\tilde{n}_u^{\text{clus}} = m - u, \quad b_u^{\text{clus}} = \min(b, B_{\text{max}}/l), \quad V_u^{\text{clus}} = 1. \quad (38)$$

Remark 1: From (19), (22), (32), and (33), and considering expressions (35) through (38), it follows that P_{UF_u} and $E(Q_{\text{UF}_u})$ are mainly determined by the term $(\lambda c/b)^{u-d-1}$, and P_{DF} and $E(Q_{\text{DF}})$ by the term $(\lambda c/b)^{\tilde{r}-d-1}$. According to (7), $\lambda c/b \ll 1$, such that, for fixed values of \tilde{r} and u , increasing d causes these parameters to increase. Therefore, by virtue of (23) and (34), increasing d causes MTTDL to decrease and EAFDL to increase. Consequently, for fixed values of m and l , deferring rebuilds degrades reliability.

D. Equivalent Systems

We call *equivalent systems* those that employ a given codeword length m and have the same number $m-l-d$ of exposure levels at which the rebuild process is active. In this case, it holds that $l+d=z$, and from (3) and (4), it follows that

$$0 \leq d < z < m \quad \text{and} \quad d+1 \leq u \leq m-z+d+1. \quad (39)$$

Next, we compare the MTTDL and EAFDL of equivalent systems. For $P_s = 0$, substituting (12), (19), and (22) into (23) yields

$$\frac{\text{MTTDL}(d+1)}{\text{MTTDL}(d)} \approx \frac{E(T|d+1)}{E(T|d)} \cdot \frac{1}{\prod_{u=d+1}^{m-z+d} V_u} \cdot \frac{\prod_{i=d+1}^{m-z+d} \frac{\tilde{n}_i(d)}{b_i(d)}}{\prod_{i=d+2}^{m-z+d+1} \frac{\tilde{n}_i(d+1)}{b_i(d+1)}}. \quad (40)$$

From (12), it follows that $E(T|d+1) > E(T|d)$. Also, V_u represent fractions, which implies that $V_u \leq 1$. Consequently, the product of the first two terms of (40) is greater than 1.

For a symmetric placement scheme that is not bandwidth constrained, it follows from (36) that $\tilde{n}_u(d)/b_u(d) = (l+1)/b = (z-d+1)/b$. Substituting this into (40) yields

$$\frac{\text{MTTDL}(d+1)}{\text{MTTDL}(d)} \approx \frac{E(T|d+1)}{E(T|d)} \cdot \prod_{u=d+1}^{m-z+d} V_u^{-1} \cdot \left(\frac{z-d+1}{z-d}\right)^{m-z} > 1. \quad (41)$$

For a clustered placement scheme that is not bandwidth constrained, it follows from (38) that $\tilde{n}_u(d)/b_u(d) = (m-u)/b$. Substituting this into (40), and using (38), yields

$$\frac{\text{MTTDL}(d+1)}{\text{MTTDL}(d)} \approx \frac{E(T|d+1)}{E(T|d)} \cdot \frac{m-d-1}{z-d-1} > 1. \quad (42)$$

Similarly, from (32) it follows that

$$\frac{E(Q_{\text{UF}_{u+1}|d+1})}{\frac{l_{d+1} E(T|d+1)}{l_d E(T|d)}} \approx \frac{E(T|d)}{E(T|d+1)} \cdot \frac{\tilde{r}(d+1)}{\tilde{r}(d)} \cdot \prod_{i=d+1}^u V_i \cdot \frac{z-d-1}{m-u} \cdot A, \quad (43)$$

$$\text{where } A = \begin{cases} \left(\frac{z-d}{z-d+1}\right)^{u-d-1}, & \text{for symmetric placement} \\ \frac{m-u}{m-d-1}, & \text{for clustered placement} \end{cases}. \quad (44)$$

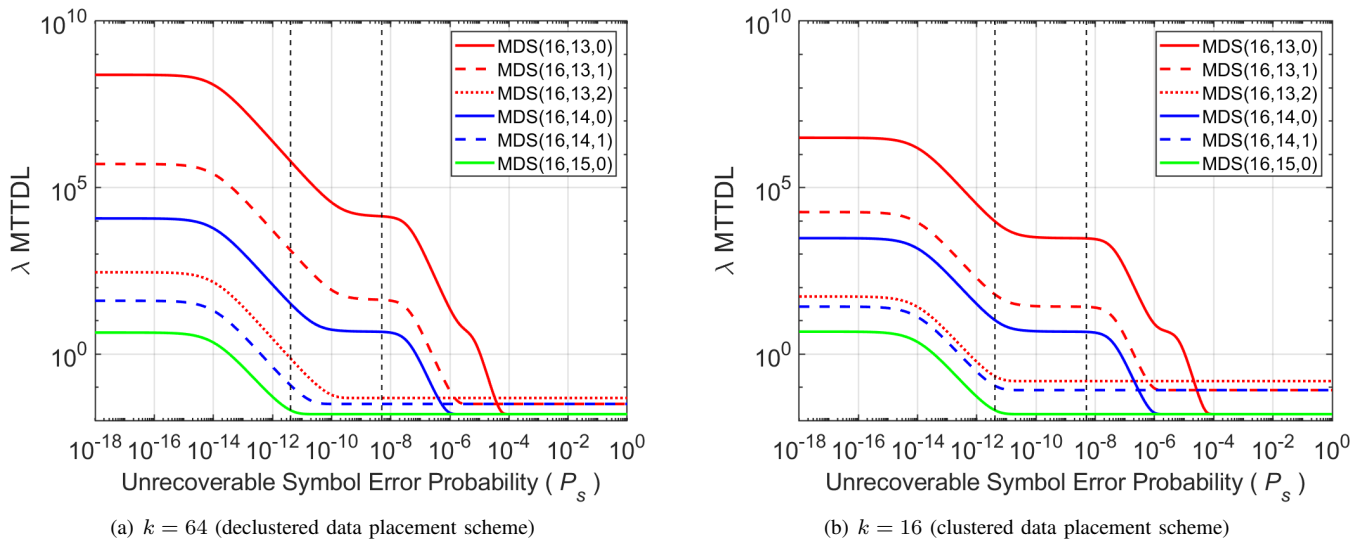

 Figure 1. Normalized MTTDL vs. P_s for various $MDS(m, l, d)$ codes ; $n = 64$, $\lambda/\mu = 0.0002$, $c = 12$ TB, and $s = 512$ B.

TABLE II. TYPICAL VALUES OF DIFFERENT PARAMETERS

Parameter	Definition	Values
n	number of storage devices	64
c	amount of data stored on each device	12 TB
l	user-data symbols per codeword	13, 14, 15
m	symbols per codeword	16
s	symbol (sector) size	512 B
b	rebuild bandwidth per device	50 MB/s
λ^{-1}	mean time to failure of a storage device	300,000 h to 1,000,000 h
U	amount of user data stored in the system	624 to 720 TB
μ^{-1}	time to read an amount c of data at a rate b from a storage device	66.7 h

It can be shown that $\frac{E(T|d)}{E(T|d+1)} \cdot \frac{\bar{r}(d+1)}{\bar{r}(d)} < 1$. Consequently, from (34), (39), and (43), and recognizing that $A < 1$ and $E(Q_{DF}) = E(Q_{UF_r})$, it follows that

$$\frac{\text{EAFDL}(d+1)}{\text{EAFDL}(d)} < 1. \quad (45)$$

Remark 2: Within the class of equivalent systems, according to (42) and (45), deferring rebuilds improves reliability, despite the fact that rebuilds are performed at the same number of exposure levels. This is because increasing d amounts to decreasing l , and therefore at a reduced number of symbols read at each exposure level. This in turn results in reduced vulnerability window and therefore improved reliability.

IV. NUMERICAL RESULTS

Here, we assess the reliability of the clustered and declustered schemes for a system comprised of $n = 64$ devices (disks), where each device stores an amount $c = 12$ TB, and $m = 16$, $l = 13, 14$, and 15 , and the symbol size s is equal to a sector size of 512 bytes.

Typical parameter values are listed in Table II. The Annualized Failure Rate (AFR) is in the range of 0.9% to 3%, which corresponds to a mean time to failure in the range of 300,000 h to 1,000,000 h. The parameter λ^{-1} is chosen to be equal to 300,000 h. It is assumed that the reserved rebuild bandwidth b is equal to 50 MB/s, which yields a rebuild time of a device $\mu^{-1} = c/b = 66.7$ h, and that the network rebuild bandwidth

is sufficiently large ($B_{\max} \geq nb = 3.2$ GB/s). We assume that the rebuild time distribution is deterministic, such that $E(X^k) = [E(X)]^k$. The obtained results are accurate because (7) is satisfied, given that $\lambda/\mu = 2.2 \times 10^{-4} \ll 1$.

First, we assess the reliability for the declustered placement scheme ($k = n = 64$) for various MDS-coded configurations with $m = 16$ and varying values of l and d . These configurations are denoted by $MDS(m, l, d)$ and the corresponding results are shown in Figures 1, 2, and 3 by solid lines for $d = 0$ (no lazy rebuild employed), dashed lines for $d = 1$ and dotted lines for $d = 2$. Six configurations are considered: $MDS(16, 13, 0)$, $MDS(16, 13, 1)$, $MDS(16, 13, 2)$, $MDS(16, 14, 0)$, $MDS(16, 14, 1)$, and $MDS(16, 15, 0)$, for each of the declustered and clustered data placement schemes. In particular, for the clustered placement scheme, the $MDS(16, 15, 0)$ and $MDS(16, 14, 0)$ configurations correspond to the RAID-5 and RAID-6 systems.

The normalized λ MTTDL measure is obtained from (13) as a function of P_s and shown in Figure 1(a) for the declustered data placement scheme. We observe that MTTDL decreases monotonically with P_s and exhibits $m - l - d$ plateaus. In the interval $[4.096 \times 10^{-12}, 5 \times 10^{-9}]$ of practical importance for P_s , which is indicated between the two vertical dashed lines, MTTDL is degraded by orders of magnitude. Increasing the number of parities (reducing l) improves reliability by orders of magnitude. By contrast, and according to Remark 1, employing lazy rebuild degrades reliability by orders of magnitude. Moreover, for equivalent systems, such as $MDS(16, 15, 0)$, $MDS(16, 14, 1)$ and $MDS(16, 13, 2)$, and according to Remark 2, MTTDL increases as d increases.

The normalized λ MTTDL measure for the clustered data placement scheme is shown in Figure 1(b). We observe that the declustered placement scheme achieves a significantly higher MTTDL than the clustered one.

The normalized EAFDL/λ measure is obtained from (14) and shown in Figure 2. We observe that EAFDL increases monotonically, but it is practically unaffected in the interval of interest because it degrades only when P_s is much larger than the typical sector error probabilities. For the EAFDL

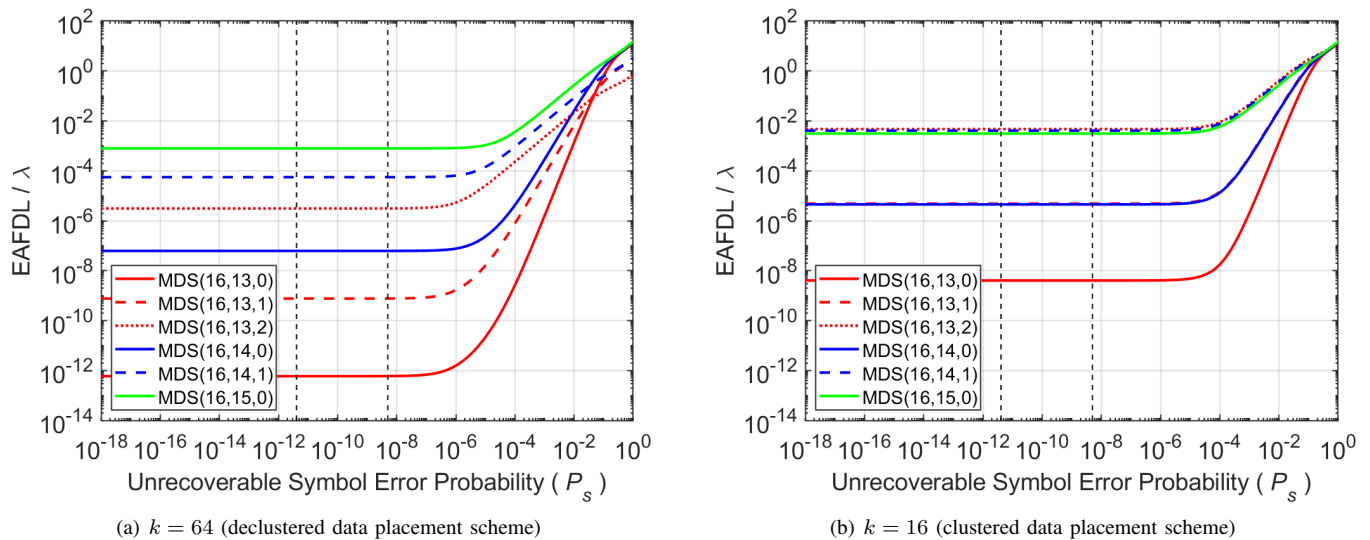


Figure 2. Normalized EAFDL vs. P_s for various MDS(m, l, d) codes ; $n = 64$, $\lambda/\mu = 0.0002$, $c = 12$ TB, and $s = 512$ B.

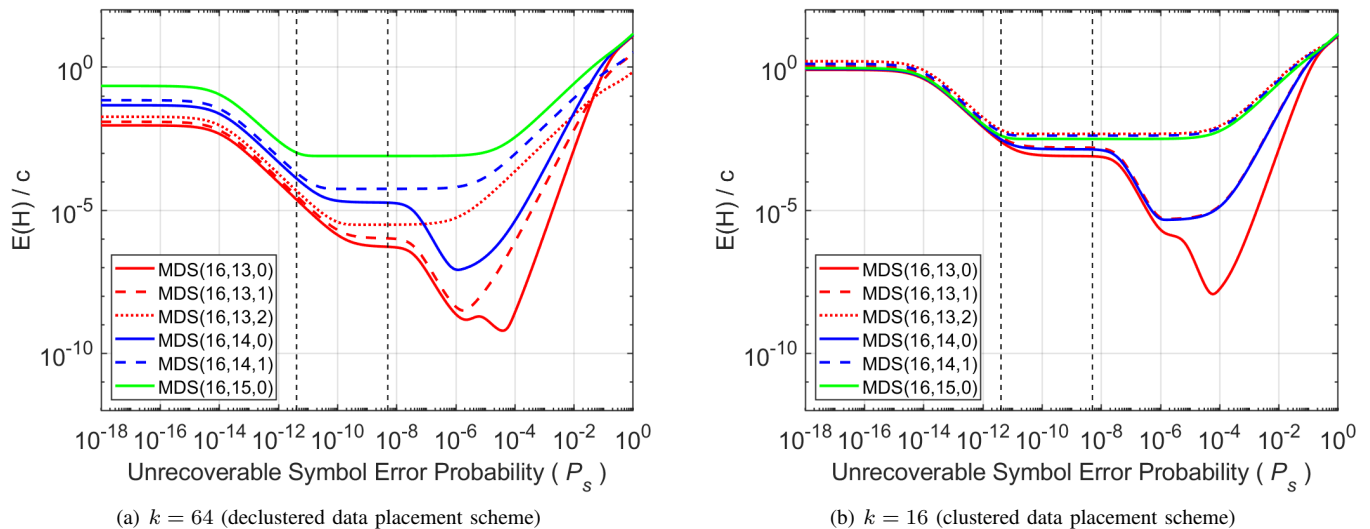


Figure 3. Normalized $E(H)$ vs. P_s for various MDS(m, l, d) codes ; $n = 64$, $\lambda/\mu = 0.0002$, $c = 12$ TB, and $s = 512$ B.

metric too, increasing the number of parities (reducing l) results in a reliability improvement by orders of magnitude. By contrast, employing lazy rebuild degrades reliability by orders of magnitude. Moreover, for equivalent systems, such as MDS(16,15,0), MDS(16,14,1) and MDS(16,13,2), and according to Remark 2, EAFDL decreases as d increases, but for the clustered placement scheme it is not significantly affected. We observe that for both MTTDL and EAFDL reliability metrics, the reliability level achieved by the declustered data placement scheme is higher than that of the clustered one.

The normalized expected amount $E(H)/c$ of lost user data, given that a data loss has occurred, relative to the amount of data stored in a device is obtained from (15) and shown in Figure 3. In contrast to the P_{DL} , EAFDL, and $E(Q)$ metrics that increase monotonically with P_s , we observe that $E(H)$ does not do so. The reason for that is the following. For $P_s \gg 10^{-14}$, data loss is more likely to be due to sector errors than to device failures. Given that sector errors result in

a negligible amount of data loss compared with the substantial data losses caused by device failures, when P_s increases over the value of 10^{-14} , the conditional amount of lost data decreases. Clearly, this is reversed for high values of P_s , and the conditional amount of lost data increases.

Also, in the interval $[4.096 \times 10^{-12}, 5 \times 10^{-9}]$ of practical importance for P_s , and by contrast to MTTDL and EAFDL, employing lazy rebuild does not affect $E(H)$ significantly. Moreover, for equivalent systems, such as MDS(16,15,0), MDS(16,14,1) and MDS(16,13,2), and for higher values of d , $E(H)$ is lower for the declustered data placement scheme, but it is not significantly affected for the clustered one.

V. CONCLUSIONS

The effect of the lazy rebuild scheme on the reliability of erasure-coded data storage systems was investigated. A methodology was developed for deriving the Mean Time to Data Loss (MTTDL) and the Expected Annual Fraction of

Data Loss (EAFDL) reliability metrics analytically. Closed-form expressions capturing the effect of unrecoverable latent errors were obtained for the symmetric, clustered and declustered data placement schemes. We demonstrated that system reliability is significantly degraded by the employment of the lazy rebuild scheme. We also demonstrated that the declustered placement scheme offers superior reliability in terms of both metrics. We established that, for realistic unrecoverable sector error rates, MTTDL is adversely affected by the presence of latent errors, whereas EAFDL is not. The analytical reliability expressions derived here can identify lazy rebuild schemes that reduce the volumes of repair traffic and at the same time ensure a desired level of reliability.

Applying these results to assess the effect of network rebuild bandwidth constraints is a subject of further investigation. The reliability evaluation of erasure-coded systems when device failures, as well as unrecoverable latent errors are correlated is also part of future work.

APPENDIX A

Proof of Proposition 1.

We consider the direct path $\overrightarrow{UF_u} = 1 \rightarrow 2 \rightarrow \dots \rightarrow u \rightarrow UF$ and proceed to evaluate $P_{UF_u}(R_{d+1}, \vec{\alpha}_{u-1})$, the probability of entering exposure level u through vector $\vec{\alpha}_{u-1} \triangleq (\alpha_1, \dots, \alpha_{u-1})$ and given a rebuild time R_{d+1} , and then encountering an unrecoverable failure during the rebuild process at this exposure level. It follows from (16) that

$$P_{UF_u}(R_{d+1}, \vec{\alpha}_{u-1}) = P_u(R_{d+1}, \vec{\alpha}_{u-2}) \cdot P_{u \rightarrow UF}(R_{d+1}, \vec{\alpha}_{u-1}). \quad (46)$$

To evaluate the above product, we first establish the following lemma.

LEMMA 1: For $u = d + 1, \dots, \tilde{r} - 1$, it holds that

$$P_u(R_{d+1}, \vec{\alpha}_{u-2}) \approx (\lambda b_{d+1} R_{d+1})^{u-d-1} \prod_{i=d+1}^{u-1} \frac{\tilde{n}_i}{b_i} (V_i \alpha_i)^{u-1-i} \quad (47)$$

with the convention that for any integer j and for any sequence δ_i , $\prod_{i=j}^0 \delta_i \triangleq 1$.

Proof: As the rebuild times are proportional to the amount of data to be rebuilt and are inversely proportional to the rebuild rates, it holds that

$$\frac{R_{d+1}}{X} = \frac{C_{d+1}}{C} \frac{b}{b_{d+1}}, \quad (48)$$

Using (8) and (10), (48) yields

$$R_{d+1} \approx \left(\prod_{j=1}^d V_j \right) \frac{b}{b_{d+1}} X, \quad (49)$$

Also,

$$\frac{R_{u+1}}{R_u} = \frac{C_{u+1}}{C_u} \frac{b_u}{b_{u+1}}, \quad \text{for } u = d + 1, \dots, \tilde{r} - 2. \quad (50)$$

Combining (9) and (50) yields

$$R_{u+1} \approx V_u \alpha_u \frac{b_u}{b_{u+1}} R_u, \quad \text{for } u = d + 1, \dots, \tilde{r} - 2. \quad (51)$$

Repeatedly applying (51) yields

$$R_u \approx \frac{b_{d+1}}{b_u} R_{d+1} \prod_{j=d+1}^{u-1} V_j \alpha_j, \quad u = d + 1, \dots, \tilde{r} - 1. \quad (52)$$

We denote by \tilde{n}_u the number of devices at exposure level u whose failure causes an exposure level transition to level $u + 1$. Subsequently, the transition probability $P_{u \rightarrow u+1}$ from exposure level u to $u + 1$ depends on the duration of the corresponding rebuild time R_u and the aggregate failure rate of these \tilde{n}_u highly reliable devices, and is given by [19]

$$P_{u \rightarrow u+1} \approx \tilde{n}_u \lambda R_u, \quad \text{for } u = d + 1, \dots, \tilde{r} - 1. \quad (53)$$

Substituting (52) into (53) yields

$$P_{u \rightarrow u+1}(R_{d+1}, \vec{\alpha}_{u-1}) \approx \tilde{n}_u \lambda \frac{b_{d+1}}{b_u} R_{d+1} \prod_{j=d+1}^{u-1} V_j \alpha_j. \quad (54)$$

The probability P_u of entering exposure level u can be approximated by the probability of the direct path $d + 1 \rightarrow d + 2 \rightarrow \dots \rightarrow u$ of successive transitions from exposure level $d + 1$ to u , that is,

$$P_u \approx \prod_{i=d+1}^{u-1} P_{i \rightarrow i+1}, \quad \text{for } u = d + 2, \dots, \tilde{r}. \quad (55)$$

Substituting (54) into (55), and using the fact that $P_{d+1} = 1$, yields (47). \blacksquare

Given that the elements of $\vec{\alpha}_{u-2}$ are independent random variables approximately distributed according to (8), such that $E(\alpha_i^k) \approx 1/(k + 1)$ for $i \geq d + 1$, we have

$$\begin{aligned} E \left(\prod_{i=d+1}^{u-1} \alpha_i^{u-1-i} \right) &= \prod_{i=d+1}^{u-1} E(\alpha_i^{u-1-i}) \\ &\approx \prod_{i=d+1}^{u-1} \frac{1}{u-i} = \frac{1}{(u-d-1)!}. \end{aligned} \quad (56)$$

Unconditioning (47) on $\vec{\alpha}_{u-2}$ and using (56) yields

$$P_u(R_{d+1}) \approx \frac{(\lambda b_{d+1} R_{d+1})^{u-d-1}}{(u-d-1)!} \prod_{i=d+1}^{u-1} \frac{\tilde{n}_i}{b_i} V_i^{u-1-i}. \quad (57)$$

Unconditioning (57) on R_{d+1} and using (6) and (49) yields (17).

We now proceed to calculate $P_{u \rightarrow UF}(R_{d+1}, \vec{\alpha}_{u-1})$. Upon entering exposure level u , the rebuild process attempts to restore the C_u most-exposed codewords, each of which has $m - u$ remaining symbols. The probability q_u that a codeword can be restored is determined by (21), which is Equation (16) of [9]. Note that, if a codeword is corrupted, then at least one of its l user-data symbols is lost. Owing to the independence of symbol errors, codewords are independently corrupted. Consequently, the conditional probability $P_{UF|C_u}$ of encountering an unrecoverable failure during the rebuild process of the C_u codewords is

$$P_{UF|C_u} = 1 - q_u^{C_u}, \quad \text{for } u = d + 1, \dots, \tilde{r}. \quad (58)$$

Substituting (10) into (58) and using (20) yields

$$P_{u \rightarrow UF}(R_{d+1}, \vec{\alpha}_{u-1}) \approx 1 - q_u^{C \prod_{j=1}^{u-1} V_j \alpha_j} = 1 - \hat{q}_u^{\prod_{j=1}^{u-1} \alpha_j}. \quad (59)$$

Substituting (59) into (46) yields

$$P_{UF_u}(R_{d+1}, \vec{\alpha}_{u-1}) \approx P_u(R_{d+1}, \vec{\alpha}_{u-2}) \left[1 - \hat{q}_u^{\prod_{j=1}^{u-1} \alpha_j} \right]. \quad (60)$$

Unconditioning (60) on $\vec{\alpha}_{u-1}$, and using (8) and (47), yields

$$P_{UF_u}(R_{d+1}) \approx P_u(R_{d+1}) - (\lambda b_{d+1} R_{d+1})^{u-d-1} \cdot \left(\prod_{i=d+1}^{u-1} \frac{\tilde{n}_i}{b_i} V_i^{u-1-i} \right) E_{\vec{\alpha}_{u-1}} \left[\left(\prod_{i=d+1}^{u-1} \alpha_i^{u-1-i} \right) \hat{q}_u^{\prod_{j=d+1}^{u-1} \alpha_j} \right]. \quad (61)$$

LEMMA 2: For α_i distributed according to (8) it holds that

$$E \left[\left(\prod_{i=d+1}^{u-1} \alpha_i^{u-1-i} \right) q^{\prod_{i=d+1}^{u-1} \alpha_i} \right] = \frac{1}{(u-d-1)!} + \log(q)^{-(u-d-1)} \left(q - \sum_{i=0}^{u-d-1} \frac{\log(q)^i}{i!} \right). \quad (62)$$

Proof: It holds that

$$q^{\prod_{i=d+1}^{u-1} \alpha_i} = e^{\log(q) \prod_{i=d+1}^{u-1} \alpha_i} = \sum_{j=0}^{\infty} \frac{\log(q)^j (\prod_{i=d+1}^{u-1} \alpha_i)^j}{j!}, \quad (63)$$

which implies that

$$\begin{aligned} & \left(\prod_{i=d+1}^{u-1} \alpha_i^{u-1-i} \right) q^{\prod_{i=d+1}^{u-1} \alpha_i} \\ &= \left(\prod_{i=d+1}^{u-1} \alpha_i^{u-1-i} \right) \left(\sum_{j=0}^{\infty} \frac{\log(q)^j (\prod_{i=d+1}^{u-1} \alpha_i)^j}{j!} \right) \\ &= \sum_{j=0}^{\infty} \frac{\log(q)^j \prod_{i=d+1}^{u-1} \alpha_i^{u-1-i+j}}{j!}. \end{aligned} \quad (64)$$

Consequently,

$$\begin{aligned} & E \left[\left(\prod_{i=d+1}^{u-1} \alpha_i^{u-1-i} \right) q^{\prod_{i=d+1}^{u-1} \alpha_i} \right] - \frac{1}{(u-d-1)!} \\ &= \sum_{j=0}^{\infty} \frac{\log(q)^j \prod_{i=d+1}^{u-1} E(\alpha_i^{u-1-i+j})}{j!} - \frac{1}{(u-d-1)!} \\ &\approx \sum_{j=0}^{\infty} \frac{\log(q)^j \prod_{i=d+1}^{u-1} E(\alpha_i^{u-1-i+j})}{j!} - \frac{1}{(u-d-1)!} \\ &\approx \sum_{j=0}^{\infty} \frac{\log(q)^j \prod_{i=d+1}^{u-1} \frac{1}{u-i+j}}{j!} - \frac{1}{(u-d-1)!} \\ &= \sum_{j=0}^{\infty} \frac{\log(q)^j}{(u-d-1+j)!} - \frac{1}{(u-d-1)!} \\ &= \sum_{j=1}^{\infty} \frac{\log(q)^j}{(u-d-1+j)!} \\ &= \log(q)^{-(u-d-1)} \sum_{i=u-d}^{\infty} \frac{\log(q)^i}{i!} \\ &= \log(q)^{-(u-d-1)} \left(\sum_{i=0}^{\infty} \frac{\log(q)^i}{i!} - \sum_{i=0}^{u-d-1} \frac{\log(q)^i}{i!} \right) \\ &= \log(q)^{-(u-d-1)} \left(e^{\log(q)} - \sum_{i=0}^{u-d-1} \frac{\log(q)^i}{i!} \right). \end{aligned} \quad (65)$$

From (57) and (62), (61) yields

$$P_{UF_u}(R_{d+1}) \approx -(\lambda b_{d+1} R_{d+1})^{u-d-1} \left(\prod_{i=d+1}^{u-1} \frac{\tilde{n}_i}{b_i} V_i^{u-1-i} \right) \cdot \log(\hat{q}_u)^{-(u-d-1)} \left(\hat{q}_u - \sum_{i=0}^{u-d-1} \frac{\log(\hat{q}_u)^i}{i!} \right). \quad (66)$$

Unconditioning (66) on R_{d+1} , and using (6) and (49), yields (19). \square

APPENDIX B

Proof of Proposition 2.

The expected number $E(S_U|C_u)$ of symbols lost due to unrecoverable failures during the rebuild of the C_u codewords at exposure level u is determined by Equation (53) of [9]:

$$E(S_U|C_u) \approx C_u \tilde{r} \binom{m-u}{\tilde{r}-u} P_s^{\tilde{r}-u}, \quad P_s \ll \frac{1}{m-\tilde{r}}. \quad (67)$$

Substituting (10) into (67) yields

$$E(S_U|\vec{\alpha}_{u-1}) \approx C \left(\prod_{j=1}^{u-1} V_j \alpha_j \right) \tilde{r} \binom{m-u}{\tilde{r}-u} P_s^{\tilde{r}-u}. \quad (68)$$

Subsequently, the expected number $E(S_{UF_u}|R_{d+1}, \vec{\alpha}_{u-1})$ of symbols lost due to unrecoverable failures encountered during rebuild in conjunction with entering exposure level u through vector $\vec{\alpha}_{u-1}$, and given a rebuild time R_{d+1} , is

$$E(S_{UF_u}|R_{d+1}, \vec{\alpha}_{u-1}) = P_u(R_{d+1}, \vec{\alpha}_{u-1}) E(S_U|\vec{\alpha}_{u-1}). \quad (69)$$

Substituting (47) and (68) into (69) yields

$$E(S_{UF_u}|R_{d+1}, \vec{\alpha}_{u-1}) \approx (\lambda b_{d+1} R_{d+1})^{u-d-1} \left[\prod_{i=d+1}^{u-1} \frac{\tilde{n}_i}{b_i} (V_i \alpha_i)^{u-i} \right] \cdot C \left(\prod_{j=1}^d V_j \right) \tilde{r} \binom{m-u}{\tilde{r}-u} P_s^{\tilde{r}-u}, \quad P_s \ll \frac{1}{m-\tilde{r}}. \quad (70)$$

Unconditioning (70) on $\vec{\alpha}_{u-1}$, and given that (56) implies that $E(\prod_{i=d+1}^{u-1} \alpha_i^{u-i}) = 1/(u-d)!$, yields

$$E(S_{UF_u}|R_{d+1}) \approx (\lambda b_{d+1} R_{d+1})^{u-d-1} \left(\prod_{i=d+1}^{u-1} \frac{\tilde{n}_i}{b_i} V_i^{u-i} \right) \frac{1}{(u-d)!} \cdot C \left(\prod_{j=1}^d V_j \right) \tilde{r} \binom{m-u}{\tilde{r}-u} P_s^{\tilde{r}-u}, \quad P_s \ll \frac{1}{m-\tilde{r}}. \quad (71)$$

Unconditioning (71) on R_{d+1} , and using (6) and (49), yields

$$E(S_{UF_u}) \approx \left(\lambda c \prod_{j=1}^d V_j \right)^{u-d-1} \frac{E(X^{u-d-1})}{[E(X)]^{u-d-1}} \left(\prod_{i=d+1}^{u-1} \frac{\tilde{n}_i}{b_i} V_i^{u-i} \right) \cdot \frac{1}{(u-d)!} C \left(\prod_{j=1}^d V_j \right) \tilde{r} \binom{m-u}{\tilde{r}-u} P_s^{\tilde{r}-u}, \quad P_s \ll \frac{1}{m-\tilde{r}}. \quad (72)$$

Substituting (72) into (31) yields (32). \square

REFERENCES

- [1] D. A. Patterson, G. Gibson, and R. H. Katz, "A case for redundant arrays of inexpensive disks (RAID)," in Proc. ACM Int'l Conference on Management of Data (SIGMOD), Jun. 1988, pp. 109–116.
- [2] P. M. Chen, E. K. Lee, G. A. Gibson, R. H. Katz, and D. A. Patterson, "RAID: High-Performance, reliable secondary storage," ACM Comput. Surv., vol. 26, no. 2, Jun. 1994, pp. 145–185.
- [3] V. Venkatesan, I. Iliadis, C. Fragouli, and R. Urbanke, "Reliability of clustered vs. declustered replica placement in data storage systems," in Proc. 19th Annual IEEE/ACM Int'l Symposium on Modeling, Analysis, and Simulation of Computer and Telecommunication Systems (MASCOTS), Jul. 2011, pp. 307–317.
- [4] I. Iliadis, D. Sotnikov, P. Ta-Shma, and V. Venkatesan, "Reliability of geo-replicated cloud storage systems," in Proc. 2014 IEEE 20th Pacific Rim Int'l Symposium on Dependable Computing (PRDC), Nov. 2014, pp. 169–179.
- [5] D. Ford et al., "Availability in globally distributed storage systems," in Proc. 9th USENIX Symposium on Operating Systems Design and Implementation (OSDI), Oct. 2010, pp. 61–74.
- [6] A. G. Dimakis, K. Ramchandran, Y. Wu, and C. Suh, "A survey on network coding for distributed storage," Proc. IEEE, vol. 99, no. 3, Mar. 2011, pp. 476–489.
- [7] C. Huang et al., "Erasure coding in Windows Azure Storage," in Proc. USENIX Annual Technical Conference (ATC), Jun. 2012, pp. 15–26.
- [8] S. Muralidhar et al., "f4: Facebook's Warm BLOB Storage System," in Proc. 11th USENIX Symposium on Operating Systems Design and Implementation (OSDI), Oct. 2014, pp. 383–397.
- [9] I. Iliadis, "Reliability assessment of erasure-coded storage systems with latent errors," in Proc. 14th Int'l Conference on Communication Theory, Reliability, and Quality of Service (CTRQ), Apr. 2021, pp. 15–24.
- [10] A. Dholakia, E. Eleftheriou, X.-Y. Hu, I. Iliadis, J. Menon, and K. Rao, "A new intra-disk redundancy scheme for high-reliability RAID storage systems in the presence of unrecoverable errors," ACM Trans. Storage, vol. 4, no. 1, 2008, pp. 1–42.
- [11] I. Iliadis, "Reliability modeling of RAID storage systems with latent errors," in Proc. 17th Annual IEEE/ACM Int'l Symposium on Modeling, Analysis, and Simulation of Computer and Telecommunication Systems (MASCOTS), Sep. 2009, pp. 111–122.
- [12] V. Venkatesan and I. Iliadis, "Effect of latent errors on the reliability of data storage systems," in Proc. 21th Annual IEEE Int'l Symposium on Modeling, Analysis, and Simulation of Computer and Telecommunication Systems (MASCOTS), Aug. 2013, pp. 293–297.
- [13] K. V. Rashmi et al., "A "Hitchhiker's" guide to fast and efficient data reconstruction in erasure-coded data centers," in Proc. 2014 ACM conference on SIGCOMM, Aug. 2014, pp. 331–342.
- [14] M. Silberstein, L. Ganesh, Y. Wang, L. Alvisi, and M. Dahlin, "Lazy means smart: Reducing repair bandwidth costs in erasure-coded distributed storage," in Proc. 7th ACM Int'l Systems and Storage Conference (SYSTOR), Jun. 2014, pp. 15:1–15:7.
- [15] I. Iliadis and V. Venkatesan, "Expected annual fraction of data loss as a metric for data storage reliability," in Proc. 22nd Annual IEEE Int'l Symposium on Modeling, Analysis, and Simulation of Computer and Telecommunication Systems (MASCOTS), Sep. 2014, pp. 375–384.
- [16] —, "Reliability evaluation of erasure coded systems," Int'l J. Adv. Telecommun., vol. 10, no. 3&4, Dec. 2017, pp. 118–144.
- [17] I. Iliadis, "Reliability evaluation of erasure coded systems under rebuild bandwidth constraints," Int'l J. Adv. Networks and Services, vol. 11, no. 3&4, Dec. 2018, pp. 113–142.
- [18] V. Venkatesan, I. Iliadis, and R. Haas, "Reliability of data storage systems under network rebuild bandwidth constraints," in Proc. 20th Annual IEEE Int'l Symposium on Modeling, Analysis, and Simulation of Computer and Telecommunication Systems (MASCOTS), Aug. 2012, pp. 189–197.
- [19] V. Venkatesan and I. Iliadis, "A general reliability model for data storage systems," in Proc. 9th Int'l Conference on Quantitative Evaluation of Systems (QEST), Sep. 2012, pp. 209–219.
- [20] DELL/EMC Whitepaper, "PowerVault ME4 Series ADAPT Software," Feb. 2019. [Online]. Available: <https://www.dellemc.com/> [retrieved: March, 2022]
- [21] I. Iliadis, R. Haas, X.-Y. Hu, and E. Eleftheriou, "Disk scrubbing versus intradisk redundancy for RAID storage systems," ACM Trans. Storage, vol. 7, no. 2, 2011, pp. 1–42.
- [22] V. Venkatesan and I. Iliadis, "Effect of codeword placement on the reliability of erasure coded data storage systems," in Proc. 10th Int'l Conference on Quantitative Evaluation of Systems (QEST), Sep. 2013, pp. 241–257.
- [23] —, "Effect of codeword placement on the reliability of erasure coded data storage systems," IBM Research Report, RZ 3827, Aug. 2012.
- [24] I. Iliadis and X.-Y. Hu, "Reliability assurance of RAID storage systems for a wide range of latent sector errors," in Proc. 2008 IEEE Int'l Conference on Networking, Architecture, and Storage (NAS), Jun. 2008, pp. 10–19.
- [25] I. Iliadis and V. Venkatesan, "Most probable paths to data loss: An efficient method for reliability evaluation of data storage systems," Int'l J. Adv. Syst. Measur., vol. 8, no. 3&4, Dec. 2015, pp. 178–200.

Explaining Radio Access Network User Dissatisfaction with Multiple Regression Models

Adrien Schaffner

LivingObjects

Toulouse, France

adrien.schaffner@livingobjects.com

Louise Travé-Massuyès

LAAS-CNRS & ANITI, University of Toulouse

Toulouse, France

louise.trave@cnrs.fr

Simon Pachy

LivingObjects

Toulouse, France

simon.pachy@livingobjects.com

Bertrand Le Marec

LivingObjects

Toulouse, France

bertrand.lemarec@livingobjects.com

Abstract—The evaluation of user satisfaction is an essential performance indicator for network operators. It can be impacted by several causes, including causes linked to the network. In addition to constantly surveying and monitoring the network, network operators count the complaints received at customer services to know the evolution of the dissatisfaction rate. The difficulty is to link the subjective comment of a customer with an objective behavior of the network. Experience shows that an indicator taken from complaints, gives a good trend on the level of network quality perceived by customers, but it is difficult to transpose into concrete actions because it is often unrelated to the key performance indicators on which engineers base their action plans. The objective of this work is to design a model that links the complaint rate, expressed by the *Customer Satisfaction Rate* indicator, with a set of key performance indicators so that performance engineers better understand customer expectations and act primarily on the indicators that give the most dissatisfaction. The model hence makes it possible to link quality of experience and quality of service.

Index Terms—Regression models, Data analysis, Knowledge extraction, Radio access networks, Quality-of-Service/Quality-of-Experience relationship, Quality via Quality-of-Experience and customer reports.

I. INTRODUCTION

In the space of a few years, the telecom market has undergone numerous technological and regulatory transformations which have engendered a price war from which operators are now trying to get out. They try to better differentiate themselves by moving towards a better customer experience and better support. The evaluation criteria most often adopted to establish a comparison of mobile networks are field measurement campaigns or user satisfaction surveys. User satisfaction surveys are expressed by the number of complaints received, the presence or absence of unfair terms in contracts, the commercial network and telephone assistance, connection time as well as call drop rate and their management noted by a supervisory authority, such as ARCEP (Regulatory Authority for Electronic Communications and Posts) in France or FCC (Federal Communications Commission) in United States.

The Customer Satisfaction Rate (CSR) is a good performance indicator that helps operators to effectively manage

and control their business and decision making. The CSR provides the number of complaints relative to the number of customers for a given area. However, predicting customer behavior, their level of satisfaction (or dissatisfaction) has always been a challenge for operators. It is therefore important to link the CSR to a set of Key Performance Indicators (KPI) that can easily be interpreted by performance engineers to act on the relevant causes of dissatisfaction. This paper presents how to learn this link from data in the form of a regression model while selecting a set of explanatory KPIs from an oversized, but yet relevant, set. The regression model captures the relationship between Quality of Experience (QoE) and Quality of Service (QoS).

The contents of the paper are organized as follows. Section II analyzes related work and positions the method of this paper with respect to the state of the art. Section III formulates the problem as a regression problem and provides the identified issues. Section IV presents two regression methods, Ordinary Least Squares (OLS) and east Absolute Shrinkage and Selection Operator (LASSO), that are later used in the method. Section V describes the application referring to explaining the customer complaint indicator CSR that has been driving the design of the method. It also presents the data that has been used and the KPIs that have been considered as candidate explanatory variables. Section VI explains the bricks of the fusion method and the fusion method itself. The results of applying the fusion method to the CSR problem are interpreted in Section VII. Finally, Section VIII concludes the paper.

II. RELATED WORK

Much research investigated about customer complaint behavior since long [1] [2]. The idea of using complaint data to solve problems in design, marketing, installation, distribution and after sale use and maintenance, is quite natural. Understanding of customer complaint and market behavior has also been investigated so as to provide a framework for interpreting the data and extrapolating it to an entire customer base [3]. Especially in the mobile telecom industry, studies on customer complaint behaviour are numerous and continue

today, significantly accentuated by the emphasis on machine learning techniques.

Given the increased competitiveness in this field, many studies have focused on a problem related to customer complaints, which is customer churn. Due to the direct effect on the revenues of the companies, especially in the telecom field, companies are seeking to develop means to predict potential customer to churn. Over the years, many machine learning algorithms have been used to produce churn prediction models and building feature's engineering and selection methods [4] [5] [6]. In the churn problem, not only complaint data but Henley segmentation, call details, line information, bill and payment information, account information, demographic profiles, service orders, etc. are potentially important. In this huge set of features, [7] identifies a subset of relevant features and applies several prediction techniques including Logistic Regressions, Multilayer Perceptron Neural Networks, Support Vector Machines and the Evolutionary Data Mining Algorithm in customer churn as predictors, based on the subset of features. [8] uses classification like the Random Forest algorithm, as well as, clustering techniques to identify the churn customers and provide the factors behind the churning of customers by categorizing the churn customers in groups.

In this paper, the focus is put on using solely complaint data to solve problems in maintenance. To do so, this work aims at linking the complaint rate with a set of technical KPIs that point at the cause of the complaints and suggest reconfiguration or repair actions on the network. This problem is much less explored in the literature than that of the churn. Literature can be exemplified by [9] that achieves correlation analysis and prediction between mobile phone users complaints and telecom equipment failures in three steps involving hierarchical clustering, pattern mining, and decision trees. On the other hand, [10] uses four machine learning algorithms, Artificial Neural Network (ANN), Support Vector Machine (SVM), K-Nearest Neighbors (KNN) and Decision Tree (DT) experimented on a database of 10,000 Korean mobile market subscribers and the variables of gender, age, device manufacturer, service quality, and complaint status. It found that ANN's prediction performance outperformed other algorithms. This last work takes into account much more data than those fixed by the objective of this paper. In addition, the first focuses on equipment failure while we want to handle the KPIs which are the data used on a daily basis by network monitoring operators. Last but not least, the algorithms used are certainly good for prediction, but they are limited in their ability to explain predictions. The relation between the prediction and the inputs of the model remains implicit. On the contrary, the objective of this work is to clearly explain this link so that it provides useful information. This is why, the approach has been based on simple regression models.

III. PROBLEM FORMULATION

Multiple linear regression [11] is a classic family of learning algorithms that postulates that a variable is expressed as the weighted sum of other variables. Multiple linear regression

defines the conditions and the model according to which a quantitative variable y is explained by several other quantitative variables $x_j, j = 1, \dots, p$. y is considered *dependent* or *endogenous* and the variables $x_j, j = 1, \dots, p$ are said to be *explanatory* or *predictor* variables. Multiple linear regression assumes that the variation of each explanatory variable has an influence, with not necessarily equal proportions, on the behavior of the dependent variable. The function that relates the dependent variable to the explanatory variables is linear.

Summarizing, multiple linear regression is a learning method that postulates that a variable y (here $y=CSR$) is expressed as the weighted sum of other variables (here the KPIs). Formally, for a number p of KPIs $x_j, j = 1, \dots, p$, the goal is to learn weights $\beta_0, \beta_1, \dots, \beta_p$ such as:

$$y = \beta_0 + \beta_1 x_1 + \dots + \beta_p x_p \quad (1)$$

For this, we have a dataset gathering n observed samples, $n > p + 1$, each of dimension $(p + 1)$ and identified by the index i :

$$(x_1^i, x_2^i, \dots, x_p^i, y^i), \quad i = 1, \dots, n, \quad (2)$$

that we use to estimate the parameters β_k ($k = 0, \dots, p$) assumed to be constant. Each sample is assumed to satisfy the relation (1) with an error ϵ_i :

$$y^i = \beta_0 + \beta_1 x_1^i + \dots + \beta_p x_p^i + \epsilon_i, \quad i = 1, \dots, n. \quad (3)$$

Under some statistical assumptions of the error terms ϵ_i , in particular independence and identical distribution, the vector of the parameters $\beta = (\beta_1, \dots, \beta_p)^T$ and the nuisance parameter σ^2 defining the variance of the error $\epsilon = (\epsilon_1, \dots, \epsilon_n)^T$, i.e., $var(\epsilon) = \sigma^2 I$, can be estimated by classical methods like least squares minimization [12] or, assuming that the error terms follow a centered normal distribution, likelihood maximization [13].

The model obtained after estimation of the parameters can be evaluated by the coefficient of determination R^2 .

$$R^2 = \frac{SSR}{SST} = \frac{\sum_i^n (\hat{y}^i - \bar{y})^2}{\sum_i^n (y^i - \bar{y})^2} \quad (4)$$

where \hat{y}^i is the prediction for the i -th sample, \bar{y} is the mean, SSR is the sum of squares due to regression, i.e., the variability from the mean \bar{y} that the regression manages to explain, and SST is the sum of squares total, i.e., the variability of the observed variables around the mean. R^2 represents the proportion of variance for the dependent variable that is explained by independent variables in the regression model. The closer the value of R^2 is to 1, the better the regression. In practice, the threshold value for R^2 for considering a good regression is highly dependent on the problem.

The goal of the obtained regression model is to extract knowledge, i.e., to determine the KPIs that influence the CSR and to quantify their influence from the coefficients of the regression.

In practice, the problems to be faced are the following :

- Business experience tells us that each of the explanatory KPIs can only worsen the condition of the telecom

network and therefore logically increases the CSR (e.g., an increase in the call drop rate, in the expert's mind, naturally increases the CSR). It is hence important to take care of the signs of the coefficients obtained by the regression.

- The number of candidate KPIs for explanation is high and can lead to irrelevant models.

IV. TWO CLASSICAL LINEAR REGRESSION METHODS

This section presents the principle of two classical multiple regression methods then leveraged in the proposed fusion method presented in Section VI.

A. Ordinary Least Squares

When trained with data, Ordinary Least Squares (OLS) method selects parameter values β_j , $j = 1, \dots, p$ of the linear expression (1) by the principle of *least squares*. It minimizes the sum of the squares of the differences between the observed dependent variable value in the data y^i , $i = 1, \dots, n$, and the value predicted by the linear function of the independent variables \hat{y}^i , $i = 1, \dots, n$. The optimization criterion, or loss function, is thus given by:

$$\begin{aligned} \mathcal{L} &= \min_{\beta_0, \beta_1, \dots, \beta_p} \sum_{i=1}^n (y^i - \hat{y}^i)^2 \\ &= \min_{\beta_0, \beta_1, \dots, \beta_n} \sum_{i=1}^n (y^i - \beta_0 - \sum_{j=1}^p x_{i,j})^2 \end{aligned} \quad (5)$$

In geometrical terms, this can be seen as the sum of the squared distances, parallel to the axis of the dependent variable, between each data point in the set and the corresponding point on the regression surface. The smaller the differences, the better the model fits the data.

The OLS estimator is consistent, i.e., has convergence to the real parameters values as the training data is increased, when the regressors are exogenous. It is optimal in the class of linear unbiased estimators when the errors are homoscedastic, i.e., they have the same variance, and are serially uncorrelated. Under these conditions, the method of OLS provides minimum-variance mean-unbiased estimation when the errors have finite variances. Under the additional assumption that the errors are normally distributed, OLS is the maximum likelihood estimator.

In this work, the function `ols` of the Python module `statsmodels` has been used to implement OLS.

B. Least Absolute Shrinkage and Selection Operator

Least Absolute Shrinkage and Selection Operator (LASSO) is a regression method that performs both variable selection and regularization in order to enhance the prediction accuracy and interpretability of the resulting model. In other words, the LASSO method handles the complexity of the model with L1 regularization [14], so that the variables not having a contribution to the model are automatically removed from the regression. This means that it adds the “absolute value of

magnitude” of coefficients as penalty term to the loss function \mathcal{L} :

$$\begin{aligned} \mathcal{L} &= \min_{\beta_0, \beta_1, \dots, \beta_p} \sum_{i=1}^n (y^i - \hat{y}^i)^2 + \lambda \sum_{j=1}^p |\beta_j| \\ &= \min_{\beta_0, \beta_1, \dots, \beta_n} \sum_{i=1}^n (y^i - \beta_0 - \sum_{j=1}^p x_{i,j})^2 + \lambda \sum_{j=1}^p |\beta_j| \end{aligned} \quad (6)$$

LASSO shrinks the less important feature's coefficients to zero thus, removing some explanatory variables altogether. This method works well for feature selection, particularly in case of a huge number of explanatory variables.

If λ is set to zero, then LASSO gets back OLS whereas a very large value increases zero coefficients hence it under-fits.

In this work, the fonction `lassocv` of the Python module `statsmodels` has been used to implement LASSO.

V. DATA AND PRE-PROCESSING

The goal is to predict the CSR and the influencing factors on a global scale, and not on each specific site, so that the operator retrieves aggregated information useful for decision making. The project was hence conducted using data at the level of French *departments* (France has 93 departments which define as many territorial communities) by setting as many regression problems as French departments.

As for the features used, the advice of telecom experts was followed and led to a mixture of signals for both 2G, 3G, and 4G for six classes: traffic (like `downlink_data_traffic`), availability (like `signaling_failure_rate`), drop rates, accessibility, performance (like `data_failure_rate`), and mobility (like `handover_drop_rate`). In total, 50 KPIs were in the list of explanatory variables, to divide between Data and Voice. Data and Voice are indeed considered to be truly independent from a customer perspective. However, the technical KPIs used by experts to explain voice and data performance have an important common basement. Among the 35 KPIs of the voice list and the 30 KPIs of the data list, 15 KPIs were common to the two lists.

The available data for each department covered a full year. While both daily and weekly values were considered, it was eventually decided to stick with daily ones, to retain a bigger dataset in the training and avoid losing information by averaging over 7 days.

In a context where the number of explanatory variables is high, it is quite often the case that several variables provide the same information or that some variables remain almost constant, or also that some variables have been poorly sensed. In order to remedy this problem, classic data pre-treatment solutions were applied in a first step resulting in:

- Removing strongly correlated variables, more precisely those with correlation coefficient higher or equal to 0.8;
- Removing variables of low variance through the dataset, more precisely those whose relative standard deviation was lower or equal to 10% of the highest;

- Removing variables with more than 10% missing values. Interpolation was used to fill the gaps for the remaining variables.

In addition, all variables were scaled so that they could be ranked according to the magnitude of their corresponding weights in the regressions.

VI. A FUSION REGRESSION METHOD WITH SELECTION OF EXPLANATORY VARIABLES

Despite the pre-processing carried out and the elimination of a subset of the KPIs proposed by experts in the field, the number of KPIs remains high, which suggests that still several of them have no direct impact on the CSR. In order to tackle this problem, the idea is to apply the following three approaches and then obtain consolidated results by fusing the results of each of them:

- Multicollinearity analysis with OLS (MCOL),
- Iterative reduction via p-value with OLS (ITER),
- Structure learning with LASSO (LASSO).

Each of the methods has its own way to tackle the problem of selecting the most relevant explanatory variables, as explained in Sections VI-A, VI-B, and VI-C. To obtain the benefits of the three methods and smooth out the inconsistencies, the three methods are then fused as explained in Section VI and illustrated in Fig. 1. This strategy follows the analysis of [15] whose results suggest the need to examine models using multiple variable selection methods, because when they do not agree, they each may expose different aspects of the complicated theoretical relationships among predictors.

Methods MCOL and ITER rely on the classical Ordinary Least Squares method (OLS) presented in Section IV-A whereas LASSO, Least Absolute Shrinkage and Selection Operator, uses the method of this name in its original version of linear regression as presented in Section IV-B.

A. Multicollinearity analysis with OLS

The MCOL method builds on OLS adding an additional preprocessing step that selects a subset of features based on multicollinearity analysis.

In a regression, multicollinearity is a problem that arises when some explanatory variables in the model measure the same phenomenon. Strong multicollinearity is problematic because it can increase the variance of the regression coefficients and make them unstable and difficult to interpret. Strongly correlated predictor coefficients will vary considerably from sample to sample. They may even present the wrong sign.

Multicollinearity does not affect the goodness of the fit or the quality of the forecast. However, the individual coefficients associated with each explanatory variable cannot be interpreted reliably whereas this interpretation is exactly what we are looking for.

Multicollinearity and correlation should not be confused. If collinear variables are de facto strongly correlated with each other, two correlated variables are not necessarily collinear. There is collinearity when two or more variables measure the "same thing".

Classically, in case of quantitative explanatory variables, multicollinearity can be assessed by the *variance inflation factor* (VIF). The VIF for an explanatory variable is equal to the ratio of the overall model variance to the variance of a model that includes only that single explanatory variable. This ratio is calculated for each explanatory variable. The VIF estimates how much the variance of a coefficient is "increased" due to a linear relationship with other predictors. Thus, a VIF of 1.7 tells us that the variance of this particular coefficient is 70% greater than the variance that should be observed if this factor was absolutely not correlated with the other predictors. The ideal case is obviously when all VIFs are equal to 1, indicating that there is no multicollinearity.

In the case study, multicollinearity analysis was performed considering the 35 and 30 KPIs indicated by the experts in the Voice and Data lists respectively. The VIF threshold was chosen to be 5, beyond which the corresponding KPI was eliminated. Fig. 2 shows the results obtained on a specific cell.

B. Iterative reduction via p-value with OLS

After training a regression model, a *p-value* for each KPI can be obtained: it tests the null hypothesis that the coefficient is equal to zero, in other words, whatever its value, the KPI brings no information whatsoever to the model. A low p-value (typically 0.05 or less) indicates that one can reject the null hypothesis: a predictor that has a low p-value is probably a meaningful addition to the model as it changes the model prediction. Conversely, a larger p-value implies that changes in the predictor do not bring changes in the response.

Whenever a new KPI is added or deleted in the training phase, the model obtained will get different regression coefficients, but also different p-values thus it makes sense to add or remove high p-value KPIs one at a time, in line with a backward elimination strategy in stepwise regression. The algorithm is then as follows:

- train a model with all KPIs,
- check which KPIs have a high p-value,
- remove the one with the highest p-value.

Although stepwise regression methods are recognized as undesirable for explanatory purposes [16] they may, however, provide efficient means to examine multiple models for further investigation.

C. Structure learning with LASSO

The lasso method is well known in the literature and has already proved itself in numerous regressions. Here is a quick reminder of the presentation of Section IV-B : in the standard regression like OLS, coefficients are obtained through minimization of the residual squared sum. The LASSO method is similar but adds a penalization term to reduce the number of KPIs kept during the regression. The penalization takes the form of an L1 norm of the coefficients which reduces the available domain of values, allowing some coefficients to be precisely zero, thus letting one remove the matching KPIs.

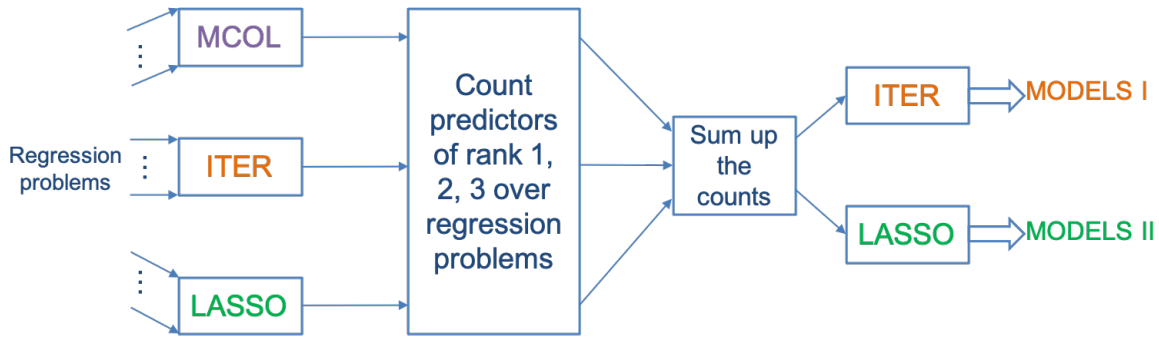


Fig. 1. Steps of the fusion regression method

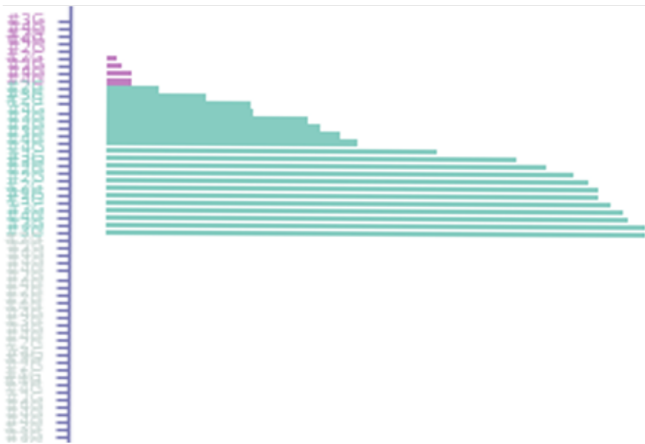


Fig. 2. KPI selection and relevancy on a specific cell: grey KPIs are those discarded by pre-processing and multicollinearity analysis, green KPIs are those of minor impact on the CSR, magenta KPIs are those that are preponderant according to the obtained regression model.

D. Fusioning the methods

In the regression model given by (1), explanatory variables $x_j, j = 1, \dots, p$, can be ranked according to the magnitude of their corresponding weight β_1, \dots, β_p . The idea developed in this work uses this ranking and includes four steps for the fusion regression method:

- Step 1 – For every regression problem, learn three regression models with the three selected methods involving explanatory variable selection, namely MCOL, ITER, and LASSO;
- Step 2 – For each method, count the number of times a given explanatory variable (KPI) has rank 1, 2, or 3 over the whole set of regression problems;
- Step 3 – Sum up the counts over the three methods and select the explanatory variables whose count exceeds a threshold \mathcal{T} ;
- Step 4 – For every regression problem, learn two regression models with ITER and LASSO considering only the explanatory variables selected at the previous step and deduce the most impacting variables and the final model.

The steps of the fusion regression method are illustrated in Fig. 1. The output of the method takes the form of two sets of models called MODELS I and MODELS II, from which knowledge about most influencing explanatory variables can be extracted as explained in Section VII.

The fusion method is exemplified with the CSR prediction problems set at the level of French departments.

Step 1-2 are illustrated in Fig. 3 that gives the results for the Voice performance problem. For each explanatory KPI, the blue, orange, and grey bars provide the number of times the KPI is ranked 1, 2 or 3 by the MCOL, ITER, and LASSO method, respectively. Let us note a good convergence of the count referring to ITER and LASSO.

Step 3 is illustrated in Fig. 4. It aggregates the counts for each method and sums them up. It hence represents the sum of the counts of the number of times an explanatory KPI is ranked 1, 2, or 3 by one of the methods MCOL, ITER, and LASSO indifferently. A threshold is chosen, here at 45, and the explanatory KPIs that count above this threshold are selected. There are 7 KPIs that count above the threshold, framed in red.

Step 4 considers the 7 "survivor" KPIs as the most relevant on the prediction of the CSR. This is why step 4 reconsiders every regression problem by restricting explanatory variables to these 7 KPIs. Only the ITER and LASSO methods are considered because of the good convergence of their results. The obtained results are provided in Fig. 5 that represents the KPIs ranked 1, 2, and 3 over ITER and LASSO and over all the French departments.

VII. MAKING SENSE OF THE PREDICTIONS

Let us recall that the objective of this work is to design a model that makes it possible to link the CSR indicator with a set of objective performance indicators so that performance engineers better understand customer expectations and act primarily on the indicators that give the most dissatisfaction. The results of the prediction problems can be analyzed in two ways: at the level of each French department, and aggregated for the whole France.

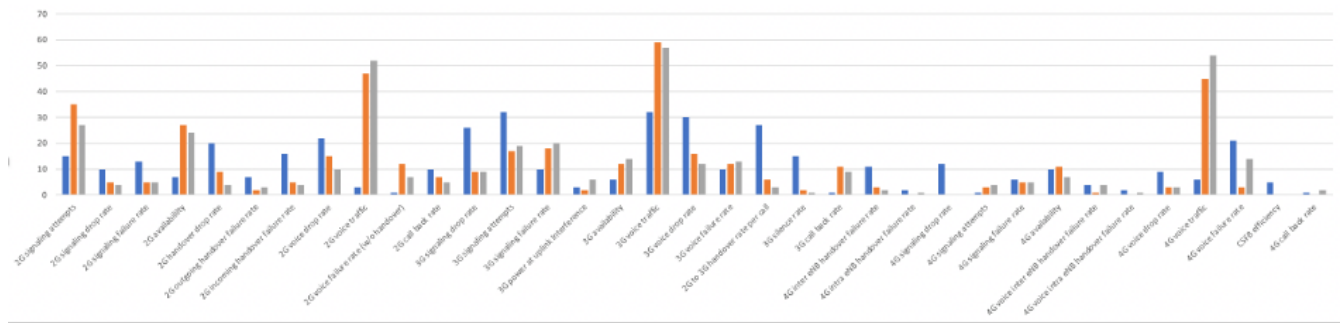


Fig. 3. Steps 1-2 of the fusion method for the Voice performance problem: count of the number of times an explanatory KPI is ranked 1, 2, or 3 by MCOL (blue), ITER (orange), LASSO (grey).

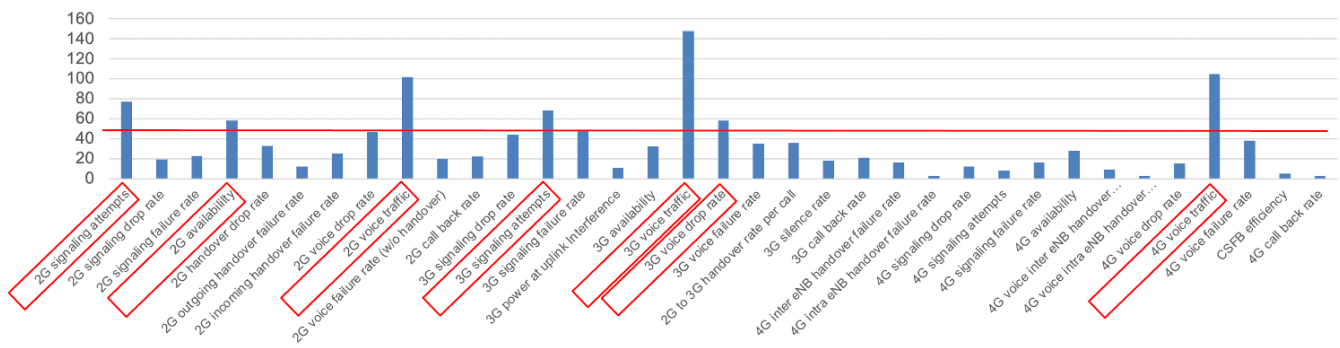


Fig. 4. Step 3 of the fusion method for the Voice performance problem: sum of the counts of the number of times an explanatory KPI is ranked 1, 2, or 3 by MCOL, ITER, LASSO. KPIs framed in red count above the threshold.

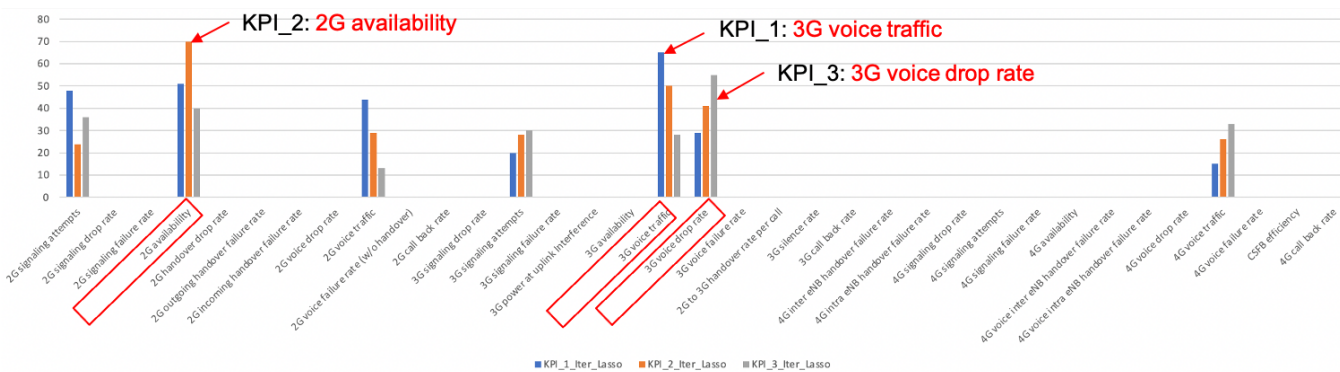


Fig. 5. KPIs ranked 1, 2, and 3 over ITER and LASSO and over all the French departments.

A. Interpretation at the level of each French department

This is done by associating a profile to each department. For this purpose, the results of the ITER method applied to the 7 survivor KPIs have been used and the department profile has been obtained by clustering the coefficients of the obtained models. This leads to the map in Fig. 6 where the departments that have similar profile are depicted with the same color. A similar profile indicates that the KPIs that must be mainly incriminated are the same, and so are the reasons explaining client complaints.

B. Aggregated interpretation

This interpretation is provided by step 4 of the fusion method. The three top KPIs over ITER and LASSO and over all the French departments appear in red in Fig. 5 and are: 3G voice traffic, 2G availability, 3G voice drop rate.

This indicates that complaints are highly related to network behavior. Among the various metrics used to measure network behavior, it appears that 2G availability that represents network maintenance processes and 3G voice drop rate that represents network call drops are the most

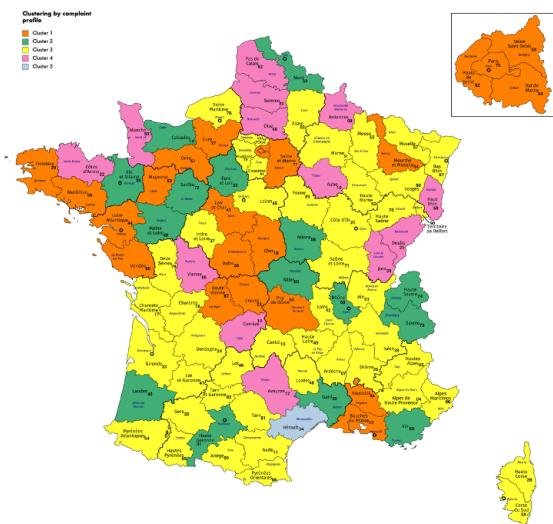


Fig. 6. Map with departments colored by profiles given by the weight of top KPIs influencing the CSR.

significant KPIs to express customer dissatisfaction, which is intuitively understandable. Traffic represented by the 3G voice traffic KPI is also a relevant metric to assess the impact of network operation on customer satisfaction. It can be related to network unavailability, loss of coverage, and network engineering issues. Let us also notice that other metrics like accessibility failure rate or mobility issues are less significant than call drops or traffic issues.

To improve client experience, the network operators should therefore prioritize to base their action plans on:

- reducing unavailability periods by, for instance, optimizing the maintenance process,
- improving the call drop rate by modifying network parameter settings, optimizing site engineering, or building new sites.

VIII. CONCLUSION AND PERSPECTIVES

This paper proposes a method to obtain a regression model with explanatory power. In many applications, the number of variables that could be thought to be explanatory for a given dependent variable is huge. However, many of them are correlated or collinear and others do not really impact the predicted variable. The method presented in this paper leverages the benefits of three methods to select relevant explanatory variables and deduce a robust regression model.

The method has been tested on telecom data to obtain a model that indicates the link of the complaint rate with a set of objective performance indicators so that performance engineers better understand customer expectations and act primarily on the indicators that give the most dissatisfaction. The final results can be used to cluster French departments according to their profile as a function of the top influencing KPIs. They can also be used on a global scale to exhibit the top KPIs at country level.

Future work will consider mapping the top KPIs returned by the model to actual actions to be performed on the network so that customer satisfaction is increased, i.e. CSR is decreased. This mapping could benefit from ideas coming from the combination of the theories of prospect theory and satisfaction games found in the literature, such as [17].

ACKNOWLEDGMENT

We would like to thank the telecom expert Didier Rana for his remarks and relevant suggestions throughout this work.

REFERENCES

- [1] J. Jacoby and J. J. Jaccard, "The sources, meaning, and validity of consumer complaint behavior: A psychological analysis." *Journal of retailing*, vol. 57, no. 3, pp. 4–24, 1981.
- [2] J. Singh and R. E. Wilkes, "When consumers complain: A path analysis of the key antecedents of consumer complaint response estimates." *Journal of the Academy of Marketing science*, vol. 24, no. 4, pp. 350–365, 1996.
- [3] J. Goodman and S. Newman, "Understand customer behavior and complaints." *Quality Progress*, vol. 36, no. 1, pp. 51–55, 2003.
- [4] W.-H. Au, K. C. Chan, and X. Yao, "A novel evolutionary data mining algorithm with applications to churn prediction." *IEEE transactions on evolutionary computation*, vol. 7, no. 6, pp. 532–545, 2003.
- [5] A. K. Ahmad, A. Jafar, and K. Aljoumaa, "Customer churn prediction in telecom using machine learning in big data platform." *Journal of Big Data*, vol. 6, no. 1, pp. 1–24, 2019.
- [6] A. Amin, F. Al-Obeidat, B. Shah, A. Adnan, J. Loo, and S. Anwar, "Customer churn prediction in telecommunication industry using data certainty." *Journal of Business Research*, vol. 94, pp. 290–301, 2019.
- [7] B. Huang, M. T. Kechadi, and B. Buckley, "Customer churn prediction in telecommunications." *Expert Systems with Applications*, vol. 39, no. 1, pp. 1414–1425, 2012.
- [8] I. Ullah, B. Raza, A. K. Malik, M. Imran, S. U. Islam, and S. W. Kim, "A churn prediction model using random forest: analysis of machine learning techniques for churn prediction and factor identification in telecom sector." *IEEE Access*, vol. 7, pp. 60 134–60 149, 2019.
- [9] Q. Yang, G. Ji, and W. Zhou, "The correlation analysis and prediction between mobile phone users complaints and telecom equipment failures under big data environments," in *2017 2nd International Conference on Advanced Robotics and Mechatronics (ICARM)*. IEEE, 2017, pp. 201–206.
- [10] C. Choi, "Predicting customer complaints in mobile telecom industry using machine learning algorithms," Ph.D. dissertation, Purdue University, 2018.
- [11] D. C. Montgomery, E. A. Peck, and G. G. Vining, *Introduction to linear regression analysis*. John Wiley & Sons, 2021.
- [12] G. S. Watson, "Linear least squares regression," *The Annals of Mathematical Statistics*, pp. 1679–1699, 1967.
- [13] I. J. Myung, "Tutorial on maximum likelihood estimation." *Journal of mathematical Psychology*, vol. 47, no. 1, pp. 90–100, 2003.
- [14] R. Tibshirani, "Regression shrinkage and selection via the lasso." *Journal of the Royal Statistical Society: Series B (Methodological)*, vol. 58, no. 1, pp. 267–288, 1996.
- [15] P. Ruengvirayudh and G. P. Brooks, "Comparing stepwise regression models to the best-subsets models, or, the art of stepwise." *General linear model journal*, vol. 42, no. 1, pp. 1–14, 2016.
- [16] G. Smith, "Step away from stepwise." *Journal of Big Data*, vol. 5, no. 1, pp. 1–12, 2018.
- [17] S. Papavassiliou, E. E. Tsiropoulou, P. Promponas, and P. Vamvakas, "A paradigm shift toward satisfaction, realism and efficiency in wireless networks resource sharing." *IEEE Network*, vol. 35, no. 1, pp. 348–355, 2020.